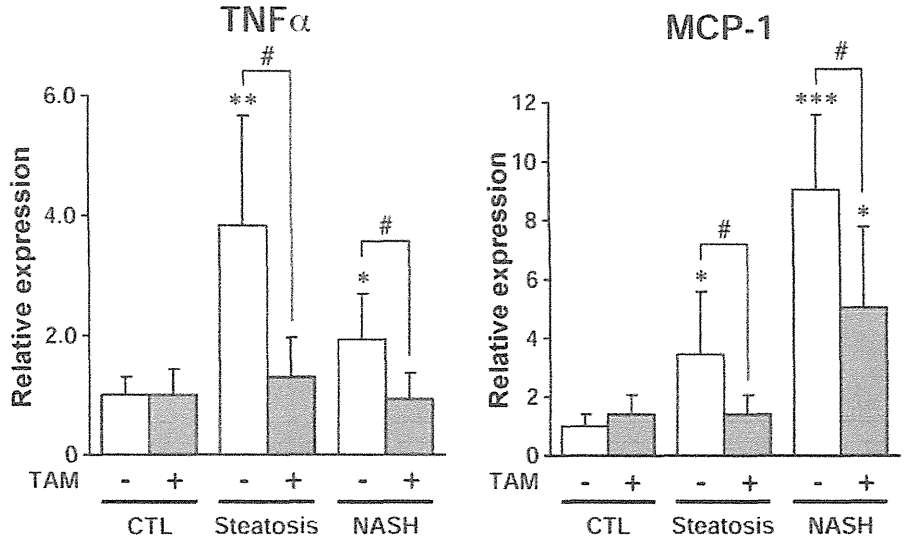

Fig. 4. Effects of tamoxifen (TAM) on hepatic mRNA expression of tumor necrosis factor α (TNFα) and monocyte chemoattractant protein-1 (MCP-1) in steatosis or non-alcoholic steatohepatitis (NASH) model mice. Mice were administered TAM for 5 days (1 mg/kg, *i.p.*). Expression of hepatic mRNA was normalized to glyceraldehyde-3-phosphate dehydrogenase (Gapdh) levels. Data are shown as the mean ± S.D. of results from 4-5 mice. Differences from the control (CTL) mice were considered significant at $^{*}p < 0.05$, $^{**}p < 0.01$ and $^{***}p < 0.001$, and differences from the TAM-unadministered model mice were considered significant at $^{\#}p < 0.05$.

2011), we confirmed that the expression levels of mRNA and proteins were similar for cytokines and chemokines. Thus, changes in mRNA levels were tracked in the present study. As shown in Fig. 4, the expression of TNFα and MCP-1 were significantly increased in the steatosis and NASH model mice compared with the CTL mice. Treatment with TAM significantly decreased TNFα and MCP-1 compared with TAM-unadministered mice (Fig. 5). These results suggested that the attenuation of liver injury by the administration of TAM is related to the decreased expression of inflammatory factors.

Effects of TAM on MAPK signaling pathways in steatosis or NASH model mice

The phosphorylation of MAPK is a major component of many intracellular signaling pathways. To clarify the MAP kinase activation status, the phosphorylation of ERK1/2 (44/42 kDa), p38 MAP kinase (43 kDa), and JNK1/2 (46/54 kDa) in liver homogenates was assessed by immunoblot analysis. No significant alteration was observed in the phosphorylation of ERK in either mouse models compared to the CTL mice. Treatment with TAM resulted in a significant increase in the ERK phosphorylation in the CTL mice and both mouse models compared with the TAM-unadministered mice. However, no change was observed in the phosphorylation of p38 in either mouse models compared with the CTL mice. In addition, treatment with TAM did not affect the phosphorylation of p38. The steatosis and NASH model mice exhibited significant increases in JNK phosphorylation compared to CTL mice. Treatment with TAM produced a significant decreased in the JNK phosphorylation in the NASH model mice compared with the TAM-unadministered mice (Fig. 5). These results suggest that the attenuation of liver injury in both mouse models by treatment with TAM is related to MAPK and ERK phosphorylation in particular.

Effects of TAM on ER stress in the liver of steatosis and NASH model mice

ER stress is caused by the accumulation of unfolded and misfolded proteins in the ER lumen and is associated with hepatic steatosis (Harding *et al.*, 2000). To investigate the mechanism of the protective effects of TAM in the mouse models, we analyzed ER stress and signaling pathways. The levels of Bip, an ER chaperone and a stress sensor protein, were increased in the liver of the steatosis and NASH model mice compared with the CTL mice. Treatment with TAM significantly decreased the

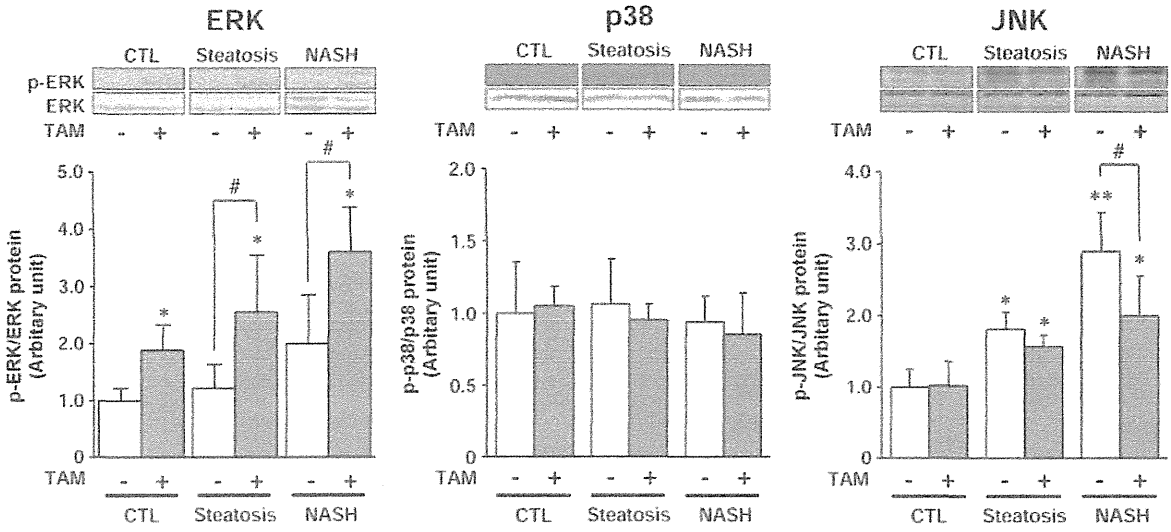

Fig. 5. Effects of tamoxifen (TAM) on mitogenactivated protein kinase (MAPK) signaling pathways in steatosis or non-alcoholic steatohepatitis (NASH) model mice. Mice were administered TAM for 5 days (1 mg/kg, *i.p.*). Liver homogenates (50 μg) were subjected to immunoblot analyses using antibodies to anti-Thr202/Thr204 phosphorylated extracellular signal-regulated kinase (ERK) 1/2, anti-Thr183/Thr185 phosphorylated c-Jun N-terminal kinase (JNK) 1/2 and anti-Thr180/Thr182 phosphorylated p38 MAPK. Data are shown as the mean ± S.D. of results from 4-5 mice. Differences from the control (CTL) mice were considered significant at $^{*}p < 0.05$, $^{**}p < 0.01$ and ***, and differences from the TAM-unadministered model mice were considered significant at $^{\#}p < 0.05$.

expression of Bip in the steatosis model mice but not in the NASH model mice compared with the TAM-unadministered mice. The levels of eIF2α, an early marker of ER stress, were increased in the NASH model mice but not in the steatosis model mice compared with the CTL mice. In addition, the levels of phosphorylated eIF2α were increased in the liver of the steatosis and NASH model mice compared with the CTL mice, whereas treatment with TAM resulted in significantly decreased eIF2α phosphorylation compared with the TAM-unadministered mice (Fig. 6). These results suggest that the attenuation of liver injury by treatment with TAM is associated with ER stress signaling.

DISCUSSION

Steatosis and NASH are now recognized as important health concerns, and their incidences have been rising. NASH develops in patients with metabolic syndrome, and can be simulated by chronic chemical intoxication as well as by the MCDD model in experimental animals. Furthermore, it is postulated that both lipid peroxidation and ROS induce the release of TNFα and MCP-1, which may contribute to NASH (Pessayre *et al.*, 2004). In general, the HFD feeding induces hepatic steatosis without progression to steatohepatitis in rodents (Vetelainen *et al.*, 2007). Estrogen has been shown to protect against HFD-induced steatosis and is suggested to play a protective role in liver injury (Riant *et al.*, 2009; Chow *et al.*, 2011). TAM is a SERM that can act as an estrogen agonist in the liver (Obsorne and Fuqua, 1994). We previously reported that TAM has a hepatoprotective effects against various drug-induced and chemical-induced acute liver injuries (Yoshikawa *et al.*, 2012). However, there is little information about the effects of TAM on steatosis and NASH. In this study, we created steatosis and NASH model mice and investigated the effects of TAM after the onset of these liver diseases. TAM decreased the plasma ALT and AST levels in both mouse models. In addition, histopathological analysis demonstrated that TAM decreased the accumulation of fat and inflammation in the livers in both mouse models. These results indicate that TAM attenuated the liver injury in the steatosis and NASH model mice.

ROS promote oxidative damage and contribute to tissue destruction in a wide variety of diseases (Te *et al.*,

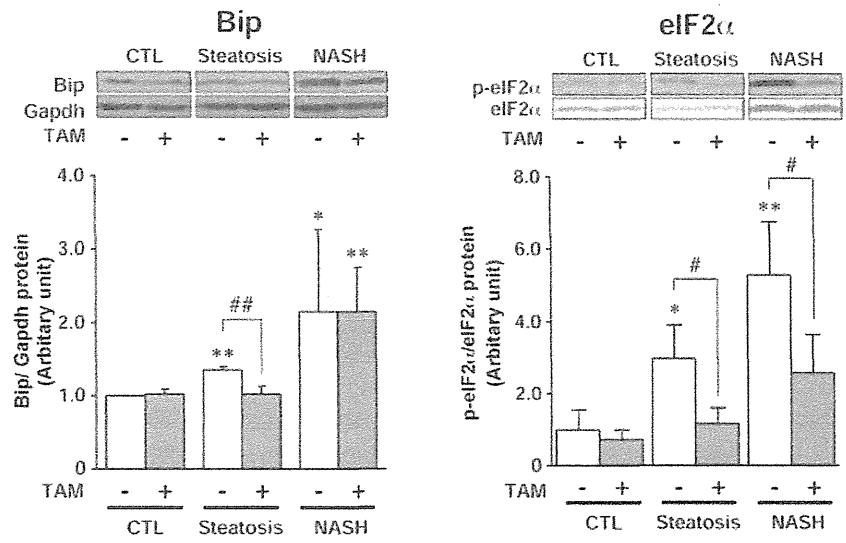

Fig. 6. Effects of tamoxifen (TAM) on endoplasmic reticulum (ER) stress in steatosis or non-alcoholic steatohepatitis (NASH) model mice. Mice were administered TAM for 5 days (1 mg/kg, *i.p.*). Liver homogenates (50 μg) were subjected to immunoblot analyses using antibodies to anti-KDEL, anti-Ser51 phosphorylated extracellular signal-regulated kinase (eIF2α) and anti- glyceraldehyde-3-phosphate dehydrogenase (Gapdh). Data are shown as the mean ± S.D. of results from 4-5 mice. Differences from the control (CTL) mice were considered significant at $^{*}p < 0.05$, $^{**}p < 0.01$ and ***, and differences from the TAM-unadministered model mice were considered significant at $^{\#}p < 0.05$.

2004). The ratios of GSH/GSSG and MDA levels are often used as a measurement of cellular toxicity and oxidative stress and appear to be increased in the progression of NAFLD (Caballero *et al.*, 2010; Chowdhry *et al.*, 2010). In the present study, the ratios of GSH/GSSG in the steatosis and NASH model mice were significantly decreased compared with CTL mice. In addition, MDA was significantly increased in both mouse models, but TAM had no effects on the ratio of GSH/GSSG or on MDA levels. These results indicated that TAM may not be involved in the oxidative stress, suggesting that another pathway may play a role in the attenuation of the liver injury in the steatosis and NASH model mice.

Fat accumulation in the liver can be recognized as the "first hit" in the pathogenesis of NASH. In addition, the fatty acid increase by the administration of TAM is considered one of the causes of steatosis (Cole *et al.*, 2010). In this study, the administration of TAM in the steatosis and NASH model mice did not change FASN and SREBP-1 levels, which are involved in fatty acid synthesis. However, administration of TAM decreased DGAT2 expression in CTL mice and both mouse models. DGAT2 is the rate-limiting enzyme catalyzing the final step in triglyceride synthesis and exerts an important role in the development of fatty liver diseases (Choi *et al.*, 2007; Yu *et al.*, 2005; Wang *et al.*, 2010). Thus, these results suggested that TAM did not increase but instead decreased the fat accumulation after the onset of steatosis and NASH.

Fatty acid β-oxidation occurs in both mitochondria and peroxisomes, where oxygen is available to enable the formation of ROS. In NASH, the fatty acid overload plays an important role in ROS generation as a result of electron leakage during mitochondrial β-oxidation in energy production (Haque *et al.*, 2010). Levels of CPT-1, a rate-limiting regulator of mitochondrial β-oxidation through its role in mitochondrial fatty acid import, were increased in the steatosis model mice, whereas administration of TAM significantly decreased CPT-1 levels compared to the TAM-unadministered mice. These results suggested that TAM may be related to the suppressed β-oxidation of fatty acid in the steatosis model mice.

Oxidative stress leads to inflammatory responses, including TNFα and MCP-1 (Hotamisligil, 2010). In addition, these proinflammatory cytokines and chemokines are associated with the development and progression of hepatic inflammation (Anstee and Goldin, 2006). The expressions of TNFα and MCP-1 were increased in the steatosis and NASH model mice. Treatment with TAM significantly decreased TNFα and MCP-1 in both mouse models compared with the TAM-unadministered mice

(Fig. 4). It has been reported that estrogen attenuates the expressions of TNFα and MCP-1via the estrogen receptor in female mice (Huang *et al.*, 2008). Thus, these results indicated that TAM would exert a hepatoprotective effect against inflammation in the steatosis and NASH model mice.

The phosphorylation of MAPK, which is required for enzyme activity, activates signaling cascades, the downstream effects of which have been linked to the regulation of cellular apoptosis, an inflammatory response (Seger and Krebs, 1995). The activation of these regulatory MAPKs such as JNK and p38, through phosphorylation, usually leads to cell death and inflammation (Martindale and Holbrook, 2002; Ura *et al.*, 2001). In contrast, MAPK family members such as ERK exert protective and anti-apoptotic effects upon activation by an upstream kinase and regulate a number of major cellular functions, such as cell proliferation, differentiation and inflammation (Czaja *et al.*, 2003). Furthermore, ERK activation is reported to decrease DGAT2 expression (Wang *et al.*, 2010; Tsai *et al.*, 2007). Increased JNK phosphorylation has been reported in steatosis and NASH model mice (Hirosumi *et al.*, 2002). Furthermore, estrogen reportedly increases ERK phosphorylation (Alvaro *et al.*, 2002). In this study, we demonstrated that TAM increased in the extent of ERK phosphorylation, which may lead to increased regeneration of the liver and reduced fat accumulation and inflammation by decreasing the expression of DGAT2, TNFα and MCP-1 in steatosis and NASH. In addition, treatment with TAM decreased JNK phosphorylation in the NASH model mice. These results suggested that ERK activation by TAM is required for the attenuation of hepatotoxicity in the steatosis and NASH model mice, and inhibition of JNK activation resulted in the attenuation of inflammation and apoptosis in NASH model mice.

It has been suggested that endoplasmic reticulum (ER) stress is associated with steatosis and NASH (Puri *et al.*, 2008; Maniratanachota *et al.*, 2005). Furthermore, apoptosis and inflammation are key features in the progression of NASH and are both linked to ER stress (Malhi and Kaufman, 2011). The accumulation of misfolded proteins in the lumen of the ER and fat accumulation activate several signaling cascades. The initial outcomes of ER signaling are the transcription of ER chaperones, such as Bip, and a reduction in protein translation, which diminishes the stress in the lumen of the ER. eIF2α expression leads to an increase in the activation of the CCAAT/enhancer binding protein (C/EBP) homologous protein (CHOP), which activates proapoptotic pathways (Ohoka *et al.*, 2005). In this study, the expression of Bip was increased by ER stress in both mouse models, whereas treatment with TAM decreased the expression of Bip in the steatosis model mice. In addition, TAM decreased eIF2α phosphorylation in both mouse models. The decrease in fat accumulation in the liver by the administration of TAM is thought to diminish ER stress, including decreasing Bip and eIF2α, leading to attenuation of the liver injury (Fig. 7).

In this study, we revealed that TAM has a protective effect on the liver injury of the steatosis and NASH model mice. However, in clinical practice, there have been reports that patients with breast cancer developed NASH upon the administration of TAM (Murata *et al.*, 2000). The causes were associated with obesity, but the detailed mechanism has not been elucidated. In addition, fatty acid increase upon the administration of TAM is considered one of the causes of steatosis (Chowdhry *et al.*, 2010). However, in this study, the administration of TAM after the onset of steatosis and NASH model mice did not increase fatty acid synthesis, but did decrease fat accumulation (Figs. 1, 3). Thus, further investigation is required to determine why the effects of TAM differ under each condition between mice and humans.

NAFLD is more common in male than female in human, which implicates estrogens as potentially protective, or indicates that androgens may aggravate NASH (Loomba *et al.*, 2009). We previously reported that TAM had hepatoprotective effects against chemical-induced acute liver injuries in female mice but not in male mice, suggesting that TAM may not affect steatosis and NASH

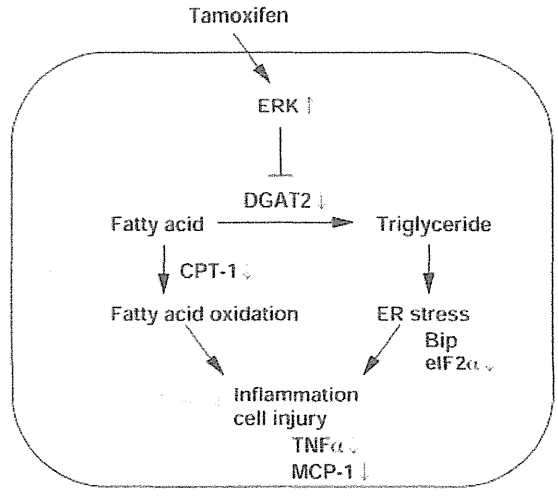

Fig. 7. Proposed mechanism of hepatoprotective effects of tamoxifen (TAM) on steatosis and non-alcoholic steatohepatitis (NASH) model mice.

model in male mice. Therefore, female mice was investigated in this study.

In conclusion, our findings clearly demonstrated that the hepatoprotective effects of TAM against steatosis and NASH are mediated through the inhibition of inflammation. Furthermore, TAM increased the activation of ERK1/2, leading to a decrease in the accumulated fat, increase in anti-apoptosis and regeneration in liver. The present study provides new information concerning the potential therapeutic effects of TAM on steatosis and NASH via activation of ERK1/2.

ACKNOWLEDGEMENTS

This study was supported by Health and Labor Sciences Research Grants from the Ministry of Health, Labor, and Welfare of Japan (H23-BIO-G001).

REFERENCES

Alvaro, D., Onori, P., Metalli, V.D., Svegliati-Baroni, G., Folli, F., Franchitto, A., Alpini, G., Mancino, M.G., Attili, A.F. and Gaudio, E. (2002): Intracellular pathways mediating estrogen-induced cholangiocyte proliferation in the rat. Hepatology, **36**, 297-304.

Angulo, P. (2002): Nonalcoholic fatty liver disease. N. Engl. J. Med., **346**, 1221-1231.

Anstee, Q.M. and Goldin, R.D. (2006): Mouse models in non-alcoholic fatty liver disease and steatohepatitis research. Int. J. Exp. Pathol., **87**, 1-16.

Caballero, F., Fernández, A., Matías, N., Martínez, L., Fucho, R., Elena, M., Caballeria, J., Morales, A., Fernández-Checa, J.C. and García-Ruiz, C. (2010): Specific contribution of methionine and choline in nutritional nonalcoholic steatohepatitis: impact on mitochondrial S-adenosyl-L-methionine and glutathione. J. Biol. Chem., **285**, 18528-18536.

Choi, C.S., Savage, D.B., Kulkarni, A., Yu, X.X., Liu, Z.X., Morino, K., Kim, S., Distefano, A., Samuel, V.T., Neschen, S., Zhang, D., Wang, A., Zhang, X.M., Kahn, M., Cline, G.W., Pandey, S.K., Geisler, J.S., Bhanot, S., Monia, B.P. and Shulman, G.I. (2007): Suppression of diacylglycerol acyltransferase-2 (DGAT2), but not DGAT1, with antisense oligonucleotides reverses diet-induced hepatic steatosis and insulin resistance. J. Biol. Chem., **282**, 22678-22688.

Chow, J.D., Jones, M.E., Prelle, K., Simpson, E.R. and Boon, W.C. (2011): A selective estrogen receptor α agonist ameliorates hepatic steatosis in the male aromatase knockout mouse. J. Endocrinol., **210**, 323-334.

Chowdhry, S., Nazmy, M.H., Meakin, P.J., Dinkova-Kostova, A.T., Walsh, S.V., Tsujita, T., Dillon, J.F., Ashford, M.L. and Hayes, J.D. (2010): Loss of Nrf2 markedly exacerbates nonalcoholic steatohepatitis. Free Radic. Biol. Med., **48**, 357-371.

Cole, L.K., Jacobs, R.L. and Vnace, D.E. (2010): Tamoxifen induces triacylglycerol accumulation in the mouse liver by activation of fatty acid synthesis. Hepatology, **52**, 1258-1265.

Cosman, F. and Lindsay, R. (1999): Selective estrogen receptor modulators: clinical spectrum. Endocr. Rev., **20**, 418-434.

Czaja, M.J., Liu, H. and Wang, Y. (2003): Oxidant-induced hepatocyte injury from menadione is regulated by ERK and AP-1 signaling. Hepatology, **37**, 1405-1413.

Dhingra, K. (1999): Antiestrogens-tamoxifen, SERMs and beyond. Invest. New Drugs, **17**, 285-311.

Donnelly, K.L., Smith, C.I., Schwarzenberg, S.J., Jessurun, J., Boldt, M.D. and Parks, E.J. (2005): Sources of fatty acids stored in liver and secreted via lipoproteins in patients with nonalcoholic fatty liver disease. J. Clin. Invest., **115**, 1343-1351.

Haque, J.A., McMahan, R.S., Campbell, J.S., Shimizu-Albergine, M., Wilson, A.M., Botta, D., Bammler, T.K., Beyer, R.P., Montine, T.J., Yeh, M.M., Kavanagh, T.J. and Fausto, N. (2010): Attenuated progression of diet-induced steatohepatitis in glutathione-deficient mice. Lab. Invest., **90**, 1704-1717.

Harada, H., Bharwani, S., Pavlick, K.P., Korach, K.S. and Grisham, M.B. (2004): Estrogen receptor-α, sexual dimorphism and reduced-size liver ischemia and reperfusion injury in mice. Pediatr. Res., **55**, 450-456.

Harding, H.P., Zhang, Y., Bertolotti, A., Zeng, H. and Ron, D. (2000): Perk is essential for translational regulation and cell survival during the unfolded protein response. Mol. Cell, **5**, 897-904.

Higuchi, S., Kobayashi, M., Yoshikawa, Y., Tsuneyama, K., Fukami, T., Nakajima, M. and Yokoi, T. (2011): IL-4 mediates dicloxacillin-induced liver injury in mice. Toxcol. Lett., **200**, 139-145.

Hirosumi, J., Tuncman, G., Chang, L., Görgün, C.Z., Uysal, K.T., Maeda, K., Karin, M. and Hotamisligil, G.S. (2002): A central role for JNK in obesity and insulin resistance. Nature, **420**, 333-336.

Hotamisligil, G.S. (2010): Endoplasmic reticulum stress and the inflammatory basis of metabolic disease. Cell, **140**, 900-917.

Huang, H., He, J., Yuan, Y., Aoyagi, E., Takenaka, H., Itagaki, T., Sannomiya, K., Tamaki, K., Harada, N., Shono, M., Shimizu, I. and Takayama, T. (2008): Opposing effects of estradiol and progesterone on the oxidative stress-induced production of chemokine and proinflammatory cytokines in murine peritoneal macrophages. J. Med. Invest., **55**, 133-141.

Jou, J., Choi, S.S. and Diehl, A.M. (2008): Mechanisms of disease progression in nonalcoholic fatty liver disease. Semin. Liver Dis., **28**, 370-379.

Kim, J.K., Fillmore, J.J., Chen, Y., Yu, C., Moore, I.K., Pypaert, M., Lutz, E.P., Kayo, Y., Velez-Carrasco, W., Goldberg, I.J., Breslow, J.L. and Shulman, G.I. (2001): Tissue-specific overexpression of lipoprotein lipase causes tissue-specific insulin resistance. Proc. Natl. Acad. Sci. USA, **98**, 7522-7527.

Kotzka, J. and Muller-Wieland, D. (2004): Sterol regulatory element-binding protein (SREBP) -1: gene regulatory target for insulin resistance? Expert Opin. Ther. Targets, **8**, 141-149.

Kuiper, G.G., Carlsson, B., Grandien, K., Enmark, E., Haggblad, J., Nilsson, S. and Gustafsson, J.A. (1997): Comparison of the ligand binding specificity and transcript tissue distribution of estrogen receptors α and β. Endocrinology, **138**, 863-870.

Loomba, R., Sirlin, C.B., Schwimmer, J.B. and Lavine, J.E. (2009): Advances in pediatric nonalcoholic fatty liver disease. Hepatology, **50**, 1282-1293.

Ludwig, J., Viggiano, T.R., McGill, D.B. and Oh, B.J. (1980): Nonalcoholic steatohepatitis. Mayo Clinic experiences with a hitherto unnamed disease. Mayo Clin. Proc. **55**, 434-438.

Malhi, H. and Kaufman, R.J. (2011): Endoplasmic reticulum stress in liver disease. J. Hepatol., **54**, 795-809.

Maniratanachota, R., Minami, K., Katoh, M., Nakajima, M. and Yokoi, T. (2005): Chaperone proteins involved in troglitazone-induced toxicity in human hepatoma cell lines. Toxicol. Sci., **83**, 293-302.

Martindale, J.L. and Holbrook, N.J. (2002): Cellular response to oxidative stress: Signaling for suicide and survival. J. Cell Physiol., **192**, 1-15.

Mitlak, B.H. and Cohen, F.J. (1997): In search of optimal long-term female hormone replacement: the potential of selective estrogen receptor modulators. Horm. Res., **48**, 155-163.

Murata, Y., Ogawa, Y., Saibara, T., Nishioka, A., Fujiwara, Y., Fukumoto, M., Inomata, T., Enzan, H., Onishi, S. and Yoshida, S. (2000): Unrecognized hepatic steatosis and non-alcoholic steatohepatitis in adjuvant tamoxifen for breast cancer patients. Oncol. Rep., **7**, 1299-1304.

Naugler, W.E., Sakurai, T., Kim, S., Maeda, S., Kim, K., Elsharkawy, A.M. and Karin, M. (2007): Gender disparity in liver cancer due to sex differences in MyD88-dependent IL-6 production. Science, **317**, 121-124.

Obsorne, C.K. and Fuqua, S.A. (1994): Mechanisms of tamoxifen resistance. Breast Cancer Res. Treat, **32**, 49-55.

Ohoka, N., Yoshii, S., Hattori, T., Onozaki, K. and Hayashi, H. (2005): TRB3, a novel ER stress-inducible gene, is induced via ATF4-CHOP pathway and is involved in cell death. EMBO J., **24**, 1243-1255.

Okabe, H., Irita, K., Taniguchi, S., Kurosawa, K., Tagawa, K., Yoshitake, J. and Takahashi, S. (1994): Endotoxin causes early changes in glutathione concentrations in rabbit plasma and liver. J. Surg. Res., **57**, 416-419.

Pessayre, D., Fromenty, B. and Mansouri, A. (2004): Mitochondrial injury in steatohepatitis. Eur. J. Gastroenterol. Hepatol., **16**, 1095-1105.

Puri, P., Mirshahi, F., Cheung, O., Natarajan, R., Maher, J.W., Kellum, J.M. and Sanyal, A.J. (2008): Activation and dysregulation of the unfolded protein response in nonalcoholic fatty liver disease. Gastroenterology, **134**, 568-576.

Riant, E., Waget, A., Cogo, H., Arnal, J.F., Burcelin, R. and Gourdy, P. (2009): Estrogens protect against high-fat diet-induced insulin resistance and glucose intolerance in mice. Endocrinology, **150**, 2109-2117.

Seger, R. and Krebs, E.C. (1995): The MAPK signaling cascade. FASEB J., **9**, 726-735.

Te Sligte, K., Bourass, K.I., Sels, J.P., Driessen, A., Stockbrugger, R.W. and Koek, G.H. (2004): Non-alcoholic steatohepatitis: Review of a growing medical problem. Eur. J. Intern. Med., **15**, 10-21.

Tsai, J., Qiu, W., Kohen-Avramoglu, R. and Adeli, K. (2007): MEK-ERK inhibition corrects the defect in VLDL assembly in HepG2 cells: potential role of ERK in VLDL-ApoB100 particle assembly. Arterioscler Thromb. Vasc. Biol., **27**, 211-218.

Tietze, F. (1969): Enzymic method for quantitative determination of nanogram amounts of total and oxidized glutathione: applications to mammalian blood and other tissues. Anal. Biochem., **27**, 502-522.

Uesugi, T., Froh, M., Arteel, G.E., Bradford, B.U. and Thurman, R.G. (2001): Toll-like receptor 4 is involved in the mechanism of early alcohol-induced liver injury in mice. Hepatology, **34**, 101-108.

Ura, S., Masuyama, H., Graves, J.D. and Gotoh, Y. (2001): MST1-JNK promotes apoptosis via caspase-dependent and independent pathways. Genes Cells, **6**, 519-530.

Vetelainen, R., van Vilet, A. and van Gulik, T.M. (2007): Essential pathogenic and metabolic differences in steatosis induced by choline or methione-choline deficient diets in a rat model. J. Gastroenterol. Hepatol., **22**, 1526-1533.

Wang, Z., Yao, T. and Song, Z. (2010): Involvement and mechanism of DGAT2 upregulation in the pathogenesis of alcoholic fatty liver disease. J. Lipid Res., **51**, 3158-3165.

Yoshikawa. Y., Miyashita. T., Higuchi. S., Tsuneyama. K., Endo. S., Tsukui. T., Toyoda. Y., Fukami. T., Nakajima. M. and Yokoi. T. (2012): Mechanisms of the hepatoprotective effects of tamoxifen against drug-induced and chemical-induced acute liver injuries. Toxicol. Appl. Pharmacol. In press.

Yu, X.X., Murray, S.F., Pandey, S.K., Booten, S.L., Bao, D., Song, X,Z., Kelly, S., Chen, S., McKay, R., Monia, B.P. and Bhanot, S. (2005): Antisense oligonucleotide reduction of DGAT2 expression improves hepatic steatosis and hyperlipidemia in obese mice. Hepatology, **42**, 362-371.

Toxicology and Applied Pharmacology 264 (2012) 42–50

Contents lists available at SciVerse ScienceDirect

Toxicology and Applied Pharmacology

journal homepage: www.elsevier.com/locate/ytaap

Mechanisms of the hepatoprotective effects of tamoxifen against drug-induced and chemical-induced acute liver injuries

Yukitaka Yoshikawa [a], Taishi Miyashita [a], Satonori Higuchi [a], Koichi Tsuneyama [b], Shinya Endo [a], Tohru Tsukui [c], Yasuyuki Toyoda [a], Tatsuki Fukami [a], Miki Nakajima [a], Tsuyoshi Yokoi [a,*]

[a] Drug Metabolism and Toxicology, Faculty of Pharmaceutical Sciences, Kanazawa University, Kakuma-machi, Kanazawa 920-1192, Japan
[b] Department of Diagnostic Pathology, Graduate School of Medicine and Pharmaceutical Science for Research, University of Toyama, Sugitani, Toyama 930-0194, Japan
[c] Research Center for Genomic Medicine, Saitama Medical University, Yamane, Hidaka 350-1241, Japan

ARTICLE INFO

Article history:
Received 28 February 2012
Revised 9 June 2012
Accepted 29 June 2012
Available online 24 July 2012

Keywords:
Monocyte to macrophage differentiation-associated 2 (Mmd2)
Estrogen receptor α
Species differences
Drug-induced liver injury
Chemical-induced liver injury

ABSTRACT

Although estrogen receptor (ER)α agonists, such as estradiol and ethinylestradiol (EE2), cause cholestasis in mice, they also reduce the degree of liver injury caused by hepatotoxicants as well as ischemia–reperfusion. The functional mechanisms of ERα have yet to be elucidated in drug-induced or chemical-induced liver injury. The present study investigated the effects of an ERα agonist, selective ER modulators (SERMs) and an ER antagonist on drug-induced and chemical-induced liver injuries caused by acetaminophen, bromobenzene, diclofenac, and thioacetamide (TA). We observed hepatoprotective effects of EE2, tamoxifen (TAM) and raloxifene pretreatment in female mice that were exposed to a variety of hepatotoxic compounds. In contrast, the ER antagonist did not show any hepatoprotective effects. DNA microarray analyses suggested that monocyte to macrophage differentiation-associated 2 (Mmd2) protein, which has an unknown function, is commonly increased by TAM and RAL pretreatment, but not by pretreatment with the ER antagonist. In ERα-knockout mice, the hepatoprotective effects of TAM and the increased expression of Mmd2 mRNA were not observed in TA-induced liver injury. To investigate the function of Mmd2, the expression level of Mmd2 mRNA was significantly knocked down to approximately 30% in mice by injection of siRNA for Mmd2 (siMmd2). Mmd2 knockdown resulted in a reduction of the protective effects of TAM on TA-induced liver injury in mice. This is the first report of the involvement of ERα in drug-induced or chemical-induced liver injury. Upregulation of Mmd2 protein in the liver was suggested as the mechanism of the hepatoprotective effects of EE2 and SERMs.

Introduction

Acetaminophen (APAP) has frequently been used in studies of drug-induced liver injury. The mechanisms of APAP-induced liver injury have become clear to some degree, but mechanisms of liver injuries caused by other drugs are not fully clarified (Bajt et al., 2008; Ganey et al., 2007; Gunawan et al., 2006).

Estradiol binds to both estrogen receptor (ER) subtypes (i.e., ERα and ERβ) with high affinity. Interestingly, ERα is highly expressed in the liver, but ERβ is not (Kuiper et al., 1997). Studies have reported that the administration of ethinylestradiol (EE2), which is an ERα agonist, at a high dose causes cholestasis in mice (Yamamoto et al., 2006); however, the administration of clinical doses of EE2 in mice have been shown to reduce the degree of liver injury caused by ischemia-reperfusion (Harada et al., 2001) and by the administration of diethylnitrosoamine (Naugler et al., 2007). Unfortunately, the functional mechanisms of ERα have not been elucidated in drug-induced and chemical-induced liver injury. Thus, the present study was designed to clarify the involvement of ERα in chemical-induced liver injuries.

Tamoxifen (TAM) and raloxifene (RAL) are selective ER modulators (SERMs) that are widely used in breast cancer treatment (Early Breast Cancer Trialists' Corroborative Group, 2005). SERMs bind to ERs as both agonists and antagonists, but their actions vary among tissues (Behjati and Frank, 2009). TAM and RAL act as ER agonists in the mammary glands, whereas they act as antagonists in bone tissue. In uterus, TAM acts as ER agonist, but RAL does not (Osborne and Fuqua, 1994). In the liver, both TAM and RAL bind to ERα as agonists (Cosman and Lindsay, 1999; Mitlak and Cohen, 1997).

We used several established hepatotoxic mouse models of drug-induced and chemical-induced liver injuries, such as APAP, bromobenzene (BB), diclofenac (DIC), and thioacetamide (TA). We selected these compounds to clarify the function of ERα in drug-induced or chemical-induced acute liver injury. Among the compounds that we chose to study, APAP is the most well-researched drug. BB and TA are metabolized by cytochrome P450 (CYP) to produce the

* Corresponding author. Fax: +81 76 234 4407.
E-mail address: tyokoi@p.kanazawa-u.ac.jp (T. Yokoi).

0041-008X/$ – see front matter © 2012 Elsevier Inc. All rights reserved.
http://dx.doi.org/10.1016/j.taap.2012.06.023

reactive metabolites (Dyroff and Neal, 1981; Koen et al., 2000; Porter et al., 1979). DIC induces liver injury in clinical practice and in studies of glutathione (GSH)-knockdown or -suppressed rodents (Harada et al., 2004; Morita et al., 2009; Purcell et al., 1991).

In the present study, we found hepatoprotective effects of TAM, EE2 and RAL in drug-induced and chemical-induced liver injuries in mice. We attempted to determine the essential factor(s) for the hepatoprotecitive effects of TAM using DNA microarray analyses and in vivo knockdown experiments.

Materials and methods

Materials. APAP, BB, DIC, ethinylestradiol (EE2), TA and TAM were obtained from Wako Pure Chemical Industries (Osaka, Japan). ICI182780 (ICI) was from TOCRIS Bioscience (Ellisville, MO), and RAL was from Toronto Research Chemicals (Tronto, Canada). AteloGene™ Systemic Use was from Koken (Tokyo, Japan), and ReverTra Ace (Moloney Murine Leukemia Virus Reverse Transcriptase RNaseH Minus) was from Toyobo (Tokyo, Japan). The siRNAs were from B-Bridge (Mountain View, CA). RNAiso, a random hexamer and SYBR Premix Ex Taq were obtained from Takara (Osaka, Japan). All of the primers were commercially synthesized at Hokkaido System Sciences (Sapporo, Japan). Other chemicals were of analytical or the highest grade commercially available.

Animals. Male and female ICR mice and C57BL/6N (6 weeks old, 20–25 g) were obtained from SLC Japan (Hamamatsu, Japan). Female ERα-knockout mice (6–8 weeks old, 20–25 g, backcrossed to C57BL/6N) were obtained from Taconic Farms (Germantown, NY). The animals were housed in a controlled environment (temperature 23 ± 1 °C, humidity 50 ± 10%, and 12 h light/12 h dark cycle) in the institution's animal facility with *ad libitum* access to food and water. The mice were acclimatized for a week before use in the experiments. Animal maintenance and treatment were performed in accordance with the National Institutes of Health Guide for Animal Welfare of Japan, and the protocols were approved by the Institutional Animal Care and Use Committee of Kanazawa University and Saitama Medical University, Japan.

Administration of TA to mice that were pretreated with EE2, TAM, RAL, or ICI. Female mice were pretreated with EE2 (100 μg/kg in saline, *i.p.*), TAM (1 mg/kg in saline, *i.p.*), RAL (3 mg/kg in saline, *i.p.*), or ICI (1 mg/kg in saline, *i.p.*) for 5 days, and TA (200 mg/kg in saline, *i.p.*) was administered 12 h after the last treatment. Twenty-four hours after the administration of TA, plasma and liver samples were collected. The liver was fixed in buffered neutral 10% formalin, embedded in paraffin, sectioned at a thickness of 2 μm, and stained with hematoxylin and eosin for microscopic examination.

Administration of hepatotoxic compounds to TAM-pretreated mice. Female mice were pretreated with TAM (1 mg/kg, *i.p.*) for 5 days. Twelve hours after the last TAM treatment, APAP (400 mg/kg in 1, 2-propanediol with 0.15% KCl, *i.p.*), BB (400 mg/kg in corn oil, *i.p.*), DIC (200 mg/kg in saline, *i.p.*), or TA (200 mg/kg in saline, *i.p.*) was administered. Plasma and liver samples were collected 6 h after the administration of APAP and DIC, or 24 h after the administration of BB and TA. In the APAP experiments, the mice were fasted for 15 h prior to the APAP administration.

Aminotransferases measurements. Plasma alanine aminotransferase (ALT), and aspartate aminotransferase (AST) were measured using a Fuji Dri-Chem 4000V (Fuji Film Med. Co., Tokyo, Japan).

DNA microarray analysis. DNA microarray analysis was performed by Hokkaido System Science (Sapporo, Japan) using a Whole Mouse Genome Oligo Microarray 44Kx4 pack (Agilent Technologies, CA). Total RNA was extracted from mouse livers using RNAiso. The quality of the total RNA samples was assessed by the 28 S/18 S rRNA ratio using an Agilent 2100 Bioanalyzer (Agilent Technologies). The RNA was amplified, converted to complementary DNA and labeled with Cy3-CTP using a Quick Amp Labeling kit (Agilent Technologies). The labeled cDNA was hybridized and the microarrays were scanned with the Agilent Technologies Microarray Scanner (Agilent Technologies) at a 5 μm resolution. The scanned data were analyzed with GeneSpring software (Agilent Technologies).

Real-time reverse transcription polymerase chain reaction (RT-PCR) analysis. Mouse Mmd2, human MMD2, mouse glyceraldehyde-3-phosphate dehydrogenase (Gapdh), and human GAPDH mRNA were quantified using real-time RT-PCR. We used the following primer sequences: mouse Mmd2, 5′-TGC TAT GTG GTG ATG GGT TTC-3′ and 5′-CTC TTA AAG AAC ACC ATG CCC-3′; human MMD2, 5′-ACC AGC CCA CAG AGT ATG AAC-3′ and 5′-CTC ACC CCA TTT GAT GTT AGT-3′; mouse Gapdh, 5′-TCA CCA GGG CTG CCA TTT G-3′ and 5′-TCC GAC AGG AAG TAG AGG TTG-3′ and human GAPDH, 5′-CCA GGG CTT TTA ACT C-3′ and 5′-GCT CCC CCC TGC CCA AAT GA-3′. For the RT step, total RNA (10 μg) and 150 ng of random hexamer were mixed and incubated at 70 °C for 10 min. An RNA solution was added to a reaction mixture containing 100 units of ReverTra Ace, reaction buffer, and 0.5 mM dNTPs in a final volume of 40 μL. The reaction mixture was incubated at 30 °C for 10 min followed by and 42 °C for 1 h and then heated at 98 °C for 10 min to inactivate the enzyme. Real-time RT-PCR was performed using an Mx3000 real-time RT-PCR system (Stratagene, La Jolla, CA). The PCR mixture contained approximately 1 μg (1 μL) of template cDNA, SYBR Premix Ex Taq solution, and 10 pmol of sense and antisense primers. We used the following PCR conditions for Mmd2, MMD2, Gapdh, and GAPDH; after an initial denaturation at 95 °C for 60 s, the amplification was performed by denaturation at 94 °C for 4 s and annealing and extension at 64 °C for 20 s (45 cycles). The amplified products were directly monitored by measuring the intensity of the SYBR Green I dye (Molecular Probes, Eugene, OR) binding to double-stranded DNA amplified by PCR.

Time-dependent changes of plasma ALT and Mmd2 mRNA in TA-administered female mice. Female mice were pretreated with TAM (1 mg/kg, *i.p.*) for 5 days, and TA (200 mg/kg, *i.p.*) was administered 12 h after the last treatment. Plasma and liver samples were collected at 0, 3, 6, 12, 24 and 48 h after TA administration.

In vivo siRNA delivery using atelocollagen. An atelocollagen-mediated siRNA delivery system was used. Atelocollagen alone, atelocollagen/siScr (a scrambled control RNA), or atelocollagen/siMmd2 (a siRNA for Mmd2, 5 nmol/mouse, *i.v.*) in a 200-μL volume was injected into the tail vein of mice. Plasma and liver samples were collected 24 h after the injection of atelocollagen. Mice were pretreated with TAM for 4 days, and atelocollagen alone, atelocollagen/siScr, or atelocollagen/siMmd2 (5 nmol/mouse, i.v.) was injected 12 h after the last TAM treatment. Twenty-four hours after the injection of the siRNA, TA (200 mg/kg, *i.p.*) was administered.

Quantitation of hepatic myeloperoxidase (MPO)-positive cells. Infiltration of mononuclear cells in the liver was assessed by immunostaining of MPO. A rabbit polyclonal antibody against MPO was used as previously described (Kumada et al., 2004). Three visuals fields of 400× magnification (0.1 mm^2) were randomly selected from each specimen and photographed by a digital camera (D-33E, OLYMPUS, Tokyo). The average number of MPO-positive mononuclear cells was compared in 5 randomly selected visual fields.

GSH assay. Total GSH (the sum of both the reduced and oxidized form) was measured using reduced GSH as the standard. Mouse liver tissue was homogenized on ice with cold 5% sulfosalicylic acid and centrifuged at 8000×*g* at 4 °C for 10 min. The resulting supernatant was diluted with distilled water, and the GSH concentration was measured as previously described (Griffith, 1980). The GSH standard curve (0.035–0.55 μmol/g protein) showed good linearity ($R^2 > 0.99$).

Human liver samples. Human liver samples from 15 donors were obtained from the Human and Animal Bridging (HAB) Research Organization (Chiba, Japan) which is in partnership with the National Disease Research Interchange (NDRI, Philadelphia, PA), and liver samples from 10 additional donors were obtained from autopsy materials that were discarded after pathological investigation. The use of the human livers was approved by the Ethics Committees of Kanazawa University (Kanazawa, Japan) and Iwate Medical University (Morioka, Japan). The subjects showed no pathological features in liver. Causes of death in subjects are summarized in Supplementary Table 1. Total RNA was extracted from the livers using RNAiso. The quality of the total RNA samples was assessed based on the 28S/18S rRNA ratio was assessed.

Statistical analysis. Statistical analyses were performed with a GraphPad Instat version 2.0 computer program (GraphPad Software, San Diego, CA). Comparisons of two groups were made with two-paired Student's *t* tests. Comparisons of multiple groups were assessed with analysis of variance (ANOVA) followed by Tukey's test. Differences compared with the control group were considered significant at $^{*}P<0.05$.

Results

Effects of EE2, TAM, RAL, and ICI on TA-induced hepatotoxicity

We investigated the effects of EE2 (ERα agonist), TAM and RAL (SERMs), and ICI (ER antagonist) on TA-induced hepatotoxicity. No significant increase of ALT or AST was observed after the treatment with EE2, TAM, RAL, or ICI alone. The plasma levels of ALT and AST, however, were dramatically increased at 24 h after TA (hepatotoxicant, 200 mg/kg, *i.p.*) administration. EE2, TAM, or RAL pretreatment significantly decreased the plasma ALT and AST levels, which were elevated by the administration of TA alone (Figs. 1A and B). In contrast, ICI pretreatment did not affect the plasma ALT and AST levels compared with the mice that were administered TA alone. Remarkable necrosis, especially around the central vein, was observed in the mice that were administered TA, but this necrosis was reduced by TAM pretreatment (Fig. 1c). The suppression of TA-induced hepatotoxicity by TAM pretreatment was also examined in male mice (Supplementary Fig. 1). Plasma ALT and AST in TAM-pretreated male mice were not different from the levels in control mice. Based on these data, we focused on the effects of TAM on drug-induced and chemical-induced liver injuries in female mice.

Effects of TAM on the hepatotoxicity induced by the various compounds

We investigated the effects of TAM pretreatment on the hepatotoxicity induced by APAP, BB and DIC (Fig. 2). Plasma ALT and AST were decreased by TAM-pretreatment in APAP-, BB-, and DIC-induced hepatotoxicity. The protective effects of TAM were commonly observed in the hepatotoxicity caused by various hepatotoxic compounds.

DNA microarray analysis

To determine the mechanism of the protective effect of TAM against the various hepatotoxic compounds, we performed a DNA microarray analysis. We analyzed the samples from mice without any pretreatment (NT), TAM alone, RAL alone, ICI alone, TA alone, TAM+TA, RAL+TA, and ICI+TA were analyzed. The EE2-pretreated sample was excluded because of the possibility that EE2 itself might cause cholestasis. Compared with the NT mice, the numbers of upregulated genes (>2-fold) in TAM alone, RAL alone, and ICI alone were 2269, 3025 and 2354, respectively. Among them, the number of upregulated genes (>2-fold) in TAM alone and RAL alone, but not in ICI, was 382. Compared with TA alone, the numbers of up-regulated genes (>2-fold) in TAM+TA, RAL+TA, and ICI+TA were 3732, 4731, and 2783, respectively. Among them, the number of upregulated genes (>2-fold) in TAM+TA and RAL+TA, but not in ICI+TA, was 968. Within the 382 and 968 genes, we found that six genes were common (Table 1). Among them, the gene that showed the highest change in the expression was monocyte to macrophage differentiation-associated 2 (Mmd2).

Compared with NT, the numbers of genes that were downregulated (<0.5-fold) in TAM alone, RAL alone, and ICI alone were 2167, 2253 and 1662, respectively. The number of genes that were downregulated (<0.5-fold) in two groups of TAM alone and RAL alone, but not in ICI alone, was 561. Compared with TA alone, the numbers of genes that were downregulated (<0.5-fold) in TAM+TA, RAL+TA, and ICI+TA were 3030, 2845, and 2225, respectively. The number of genes that were downregulated (<0.5-fold) in both groups of TAM+TA and RAL+TA, but not in ICI+TA, was 673. There were no common genes within the 561 and 673 genes.

Effects of TAM pretreatment on the time-dependent changes of plasma ALT and hepatic mRNA expression levels of 6 common genes

We investigated the time-dependent changes of plasma ALT and the hepatic mRNA of 6 common genes after TA administration with or without TAM-pretreatment. In the mice that received TAM pretreated prior to TA, the plasma ALT was significantly lower at all of the time points compared with the mice that received TA alone (Fig. 3A). In addition, the Mmd2 mRNA levels were significantly increased in the TAM-pretreated mice that received TA at all time points (Fig. 3B). The peak time of the Mmd2 mRNA showed at earlier time point than that of the plasma ALT. In contrast, the peak time of the mRNA expression of 5 genes (Pign, Mmp9, Hemt1, Arg2, and Gdf9) was the same as that of ALT (data not shown). In the TAM-pretreated mice, the expression level of Mmd2 reached its peak 3 h after TA administration (Fig. 3B), which indicated that Mmd2 expression quickly responded prior to the ALT increase. Thus, we further investigated the function of Mmd2.

Effects of TAM pretreatment on the expression level of Mmd2 mRNA in the mice that were administered with various hepatotoxic compounds

We investigated the effects of TAM pretreatment on the expression level of hepatic Mmd2 mRNA in mice that were administered various hepatotoxic compounds (Fig. 4). In the mice that were not injected with a hepatotoxic compound, the Mmd2 mRNA levels were significantly increased by TAM (6.2-fold) or RAL (14.1-fold) pretreatment. In contrast, the expression level of Mmd2 mRNA was not changed by ICI pretreatment. In the mice that were pretreated with TAM and injected with APAP, BB, DIC, or TA, Mmd2 mRNA was significantly increased compared with APAP (27-fold), BB (11-fold), DIC (84-fold), or TA (25-fold) alone (Fig. 4). Interestingly, the expression levels of Mmd2 mRNA in mice that received APAP, DIC or TA alone were lower than that in the control mice.

Effects of TAM pretreatment on TA-induced hepatotoxicity in ERα-knockout mice

Because TAM is known to bind to ERα, we investigated the effects of TAM pretreatment on TA-induced liver injury and the expression level of hepatic Mmd2 mRNA in ERα-knockout mice (Fig. 5). In C57BL/6N wildtype mice, TAM pretreatment decreased plasma ALT and AST, which were elevated by TA administration. Interestingly, the C57BL/6N wildtype mice showed significantly lower ($P<0.05$) ALT and AST levels compared with the ICR mice after TA administration (Fig. 1). In contrast, TAM pretreatment did not affect the plasma ALT, AST or the expression of Mmd2 mRNA in ERα-knockout mice. The expression level of Mmd2 mRNA was significantly lower compared with the wildtype mice. In addition, the plasma ALT and AST in the ERα-knockout mice were significantly higher than in the wildtype mice treated with TA (Fig. 5).

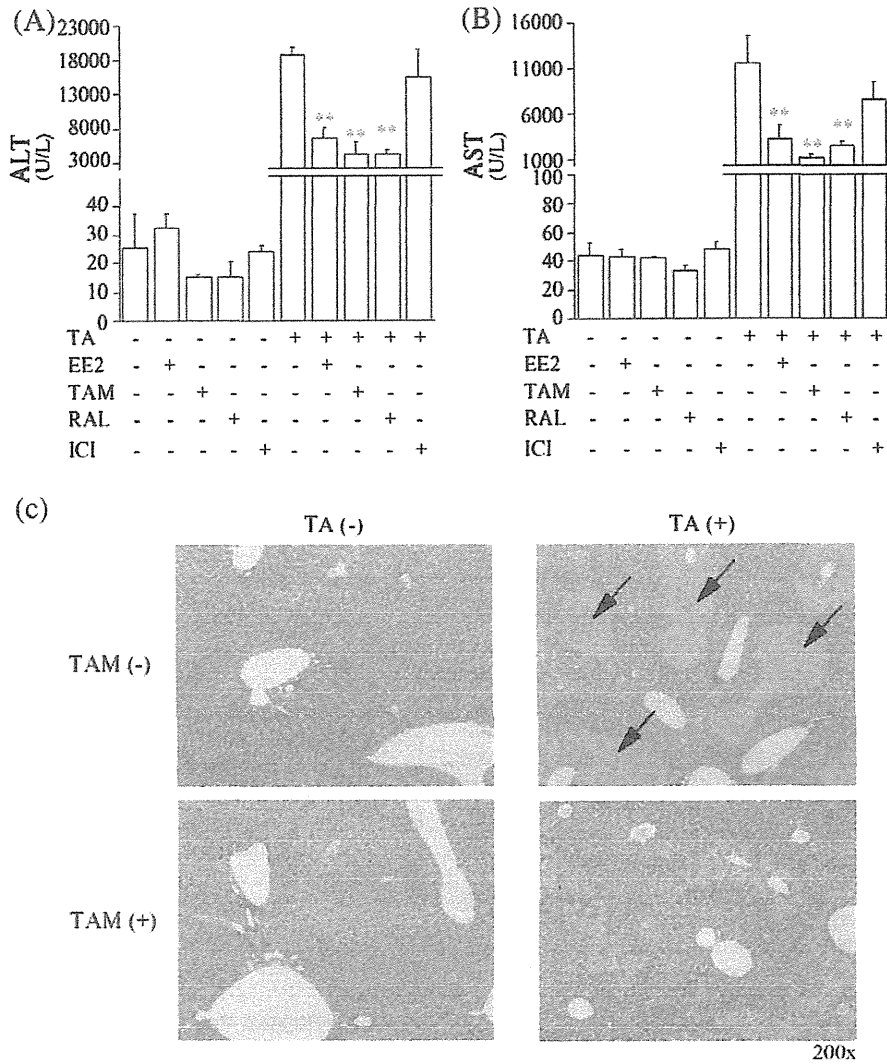

Fig. 1. The effects of EE2, TAM, RAL, and ICI on TA-induced hepatotoxicity in female mice. The mice (6 weeks old) were pretreated with EE2 (100 μg/kg, *i.p.*), TAM (1 mg/kg, i.p.), RAL (3 mg/kg, *i.p.*), or ICI (1 mg/kg, *i.p.*) for 5 days, and TA (200 mg/kg, *i.p.*) was administered 12 h after the last treatment. Twenty-four hours after the administration of TA, plasma samples were collected for assessment of the transaminase levels (A and B). Hematoxylin and eosin staining was performed on liver sections from the TAM-pretreated mice (c). Data are shown as the mean ± SD of the results from 4 mice. Differences compared with the mice that were administered TA alone were considered significant at $^{**}P<0.01$. Hepatic necrosis, which is indicated by the arrows, was only observed in the mice administered TA alone.

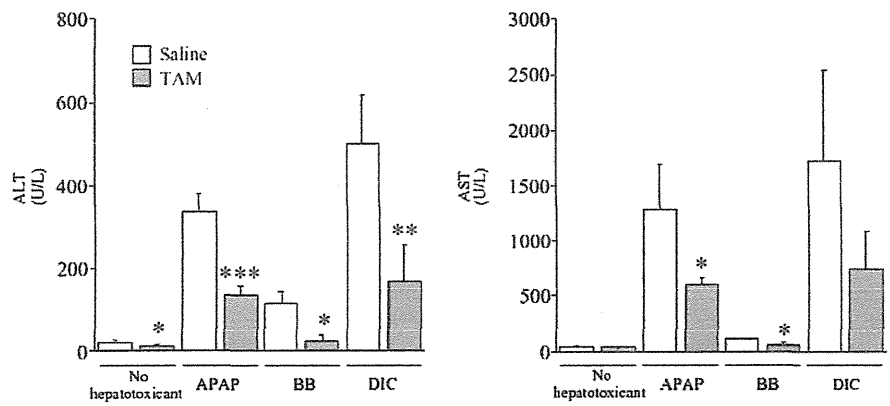

Fig. 2. The effects of TAM pretreatment on hepatotoxicity induced by various compounds in mice. The mice (6 weeks old) were pretreated with TAM (1 mg/kg, *i.p.*) for 5 days. Twelve hours after the last treatment of TAM, APAP (400 mg/kg, *i.p.*), BB (2.5 mmol/kg, *i.p.*), or DIC (200 mg/kg, *i.p.*) was administered. Six hours after the administration of APAP and DIC and 24 h after the administration of BB, plasma samples were collected for assessment of the transaminase levels. Data are shown as the mean ± SD of results from 4 mice. Differences compared with the saline-pretreated mice were considered significant at $^{*}P<0.05$, $^{**}P<0.01$, and $^{***}P<0.001$.

Table 1
Genes commonly increased by TAM and RAL pretreatment, but not ICI pretreatment, in TA-administered mice. These results are from DNA microarray analysis.

Gene name	Genbank ID	Common name	TAM*	ICI*	RAL*
Monocyte to macrophage differentiation-associated 2	NM_175217	Mmd2	7.57	1.86	8.21
Phosphatidylinositol glycan anchor biosynthesis class N	NM_013784	Pign	5.50	1.10	3.41
Matrix metallopeptidase 9	NM_013599	Mmp9	3.30	1.10	6.49
Hematopoietic cell transcript 1	NM_010416	Hemt1	3.28	1.09	2.72
Arginase 2	NM_009705	Arg2	2.67	1.08	4.74
Growth differentiation factor 9	NM_008110	Gdf9	2.02	1.09	7.38

*fold change compared with NT.

Mmd2 knockdown in cell lines

Prior to the *in vivo* experiments, we used cell lines to compare the ability of 5 types of Mmd2 siRNA (siMmd2) to knockdown Mmd2 expression to select the most effective siRNA. We measured Mmd2 mRNA expression levels in 6 different mouse cell lines (i.e., J774A.1, RAW264.7, NIH/3T3, MM45LTi, Hepa1-6, and Y-1) and found Mmd2 mRNA expression in the J774A.1 and Y-1 cell lines (Supplementary Fig. 2). The five different sequences of siMmd2 were transfected into J774A.1 and Y-1 cells (Supplementary Fig. 3). In both cell lines, Mmd2 mRNA was significantly decreased by the transfection of the #5 siMmd2. Therefore, we selected #5 siRNA for the subsequent *in vivo* experiments.

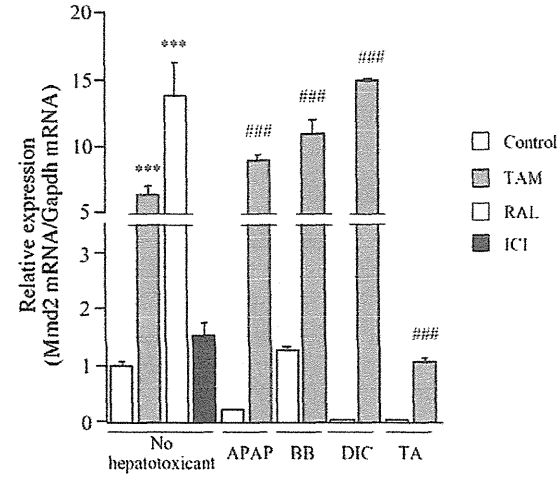

Fig. 4. The effects of various compounds on the expression level of Mmd2 mRNA in mouse liver. The mice (6 weeks old) were pretreated with TAM (1 mg/kg, *i.p.*) for 5 days. Twelve hours after the last TAM treatment, APAP (400 mg/kg, *i.p.*), BB (2.5 mmol/kg, *i.p.*), DIC (200 mg/kg, *i.p.*), or TA (200 mg/kg, *i.p.*) was administered. Six hours after the administration of APAP and DIC and 24 h after the administration of BB and TA, liver samples were collected for assessment of Mmd2 mRNA levels. Data are shown as the mean±SD of the results from 4 mice. Differences compared with the mice that were not administered a hepatotoxicant were considered significant at $^{***}P<0.001$. Differences compared with the mice that received a hapatotoxicant without TAM pretreatment were considered significant at $^{###}P<0.001$.

Effects of siMmd2 on TA-induced hepatotoxicity in mice

In vivo knockdown experiments were conducted using the #5 sequence of siMmd2 (siMmd2). The expression level of hepatic Mmd2 mRNA was significantly decreased (Fig. 6A) and the plasma ALT was slightly increased in siMmd2-injected mice compared with siScr-injected mice (Fig. 6B). The expression levels of Mmd2 mRNA and plasma ALT and AST in atelocollagen-alone or siScr-injected mice were not different from the levels in the NT mice (Figs. 6A and B). In the TAM-pretreated wildtype mice, the expression level of Mmd2 mRNA was significantly decreased by the injection of siMmd2 (Fig. 6C).

To determine the effects of the Mmd2 knockdown on the hepatoprotective effects of TAM pretreatment, siMmd2 and TA were injected in mice (Fig. 7). In the mice that received TA alone and in the TAM-pretreated mice that received TA, the plasma ALT and AST levels were significantly increased by the knockdown of siMmd2 (Figs. 7A and B). In addition, the number of MPO-positive cells was significantly increased by the knockdown of siMmd2 (Fig. 7C). Moreover, the hepatic GSH levels were significantly decreased in the mice that received TA, however, we did not observe a decrease in GSH after the knockdown of siMmd2 in the TAM-pretreated mice that received TA. Thus, Mmd2 might be one of the essential factor in the hepatoprotective effects of TAM.

Expression level of MMD2 in human liver

We compared the hepatic expression levels of human MMD2 and TAM- and TA-untreated mouse Mmd2 (Fig. 8). Interestingly, the MMD2 mRNA in human liver was markedly lower (0.1% of mouse) than the mRNA level in mouse liver.

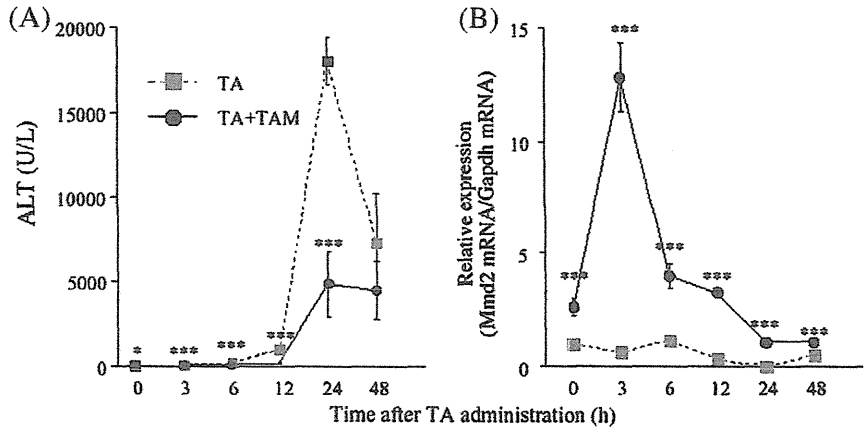

Fig. 3. Time-dependent changes of plasma ALT (A) and the expression levels of hepatic Mmd2 mRNA (B) in the mice that were pretreated with TAM or saline. The mice (6 weeks old) were pretreated with TAM (1 mg/kg, *i.p.*) for 5 days, and TA (200 mg/kg, *i.p.*) was administered 12 h after the last TAM treatment. Plasma and liver samples were collected at 0, 3, 6, 12, 24 and 48 h after the TA administration. Data are shown as the mean±SD of the results from 3 mice. Differences compared with the mice that were administered TA alone were considered significant at $^{*}P<0.05$ and $^{***}P<0.001$.

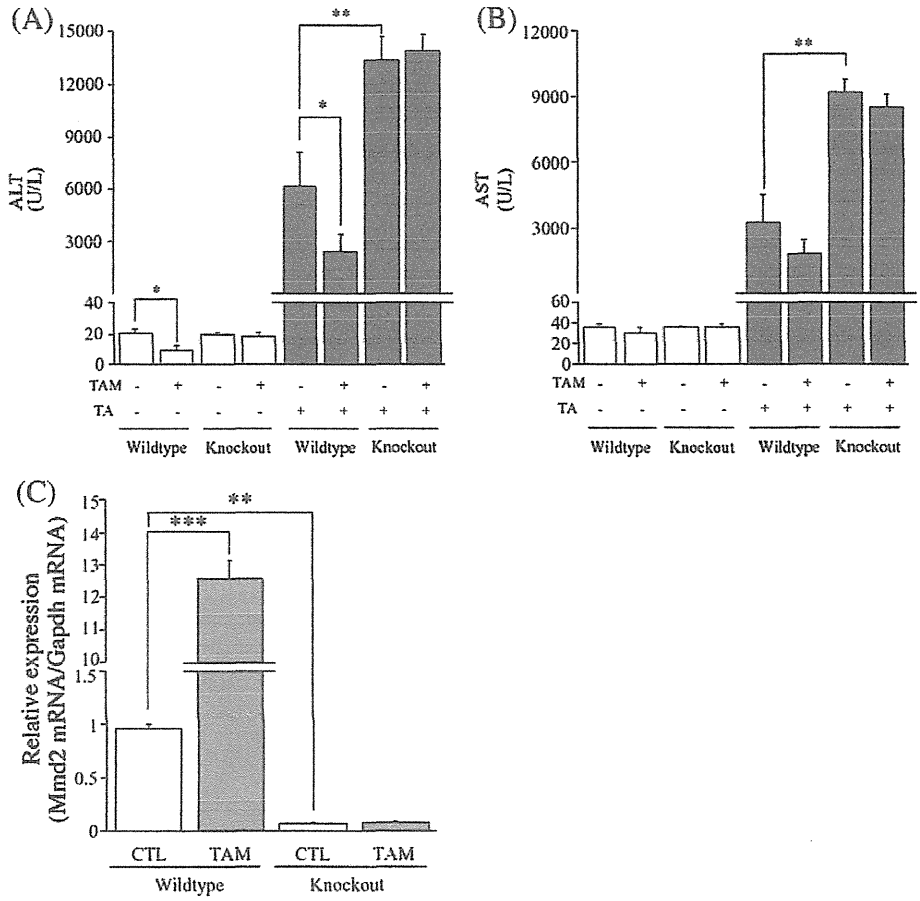

Fig. 5. The effects of TAM pretreatment on TA-induced hepatotoxicity and the expression level of hepatic Mmd2 mRNA in ERα knockout mice. The mice (female, backcrossed to C57BL/6N, 6–8 weeks old) were pretreated with TAM (1 mg/kg, *i.p.*) for 5 days, and TA (200 mg/kg, *i.p.*) was administered 12 h after the last TAM treatment. Twenty-four hours after the TA administration, plasma and liver samples were collected for assessment of the transaminase levels (A and B) and the expression level of hepatic Mmd2 mRNA (C). Wildtype C57BL/6N female mice were used as a control. Data are shown as the mean ± SD of the results from 4 mice. Differences compared with the control group were considered significant at $^{*}P<0.05$, $^{**}P<0.01$, and $^{***}P<0.001$.

Discussion

The present study demonstrated the hepatoprotective effects of EE2 (ERα agonist), TAM and RAL (SERMs) via ERα on drug-induced and chemical-induced liver injuries in mice. In addition, we demonstrated a novel mechanism by which Mmd2, which previously had an unknown function, played an essential role in the hepatoprotective effects.

Pretreatment with EE2, TAM, and RAL dramatically suppressed TA-induced hepatotoxicity in mice (Fig. 1). Interestingly, the TAM pretreatment elicited the largest decreases in ALT and AST. SERMs (TAM and RAL) are widely used in breast cancer treatment. Although EE2, TAM and RAL act as ERα agonists in the liver (Mitlak and Cohen, 1997; Cosman et al., 1999), SERMs bind to ER as both agonists and antagonists, and their actions vary among tissues (Behjati and Frank, 2009). Thus, TAM was used in the present study to investigate the hepatoprotective mechanism for drug-induced and chemical-induced liver injuries.

In the present study, we selected 4 typical hepatotoxic drugs or chemicals to examine the drug-induced and chemical-induced liver injuries. The dose and the toxic time points of TA (Kang et al., 2008), APAP (Numata et al., 2007), BB (Randle et al., 2008), and DIC (Cantoni et al., 2003) were selected based on previous reports. Hepatotoxic animal models were successfully created with the 4 hepatotoxic drugs using normal mice. The hepatoprotective effects of TAM were observed for all of the drugs and chemicals that were examined in the present study. Therefore, the hepatoprotective effects of TAM were commonly observed in hepatotoxicity caused by various hepatotoxic compounds.

Although the function of Mmd2 (Genbank ID: NM_175217) is not known, human MMD2 was recently identified to be associated with Crohn's disease by a genome-wide association study (McGovern et al., 2010). In addition, the expression of Mmd2 has been shown to be increased by HIV-1 infection in mesenchymal stem-cell-derived hematopoietic cells (Nazari-Shafti et al., 2011). In the present study, Mmd2 was identified by DNA microarray analyses from six genes that commonly increase after TAM and RAL pretreatment, but not by ICI (ER antagonist) pretreatment, in the liver of female mice administered TA. Because the plasma of EE2-pretreated mice changed to a dark yellow color after TA administration, which suggested that cholestasis had occurred, these samples were not used in the DNA microarray analyses.

The TAM-mediated suppression of TA-induced hapatotoxicity was associated with increased expression of hepatic Mmd2 in female mice. Although the expression levels of ERα and Mmd2 mRNA in the liver were similar between female and male mice, the expression level of Mmd2 was not increased by TAM pretreatment in the male mice (data not shown). No putative binding region of ERα was identified up to 4000 bp in the 5′-upstream region of the Mmd2 genes. Taken together, these results demonstrate sex differences in the hepatoprotective effects of TAM, but the underlying mechanism remains unknown.

Notably, in ERα-knockout mice, the TA-induced elevation in the plasma ALT and AST levels were not attenuated by TAM pretreatment (Fig. 5). In addition the expression level of Mmd2 mRNA in the ERα-knockout mice was considerably lower than the level in the

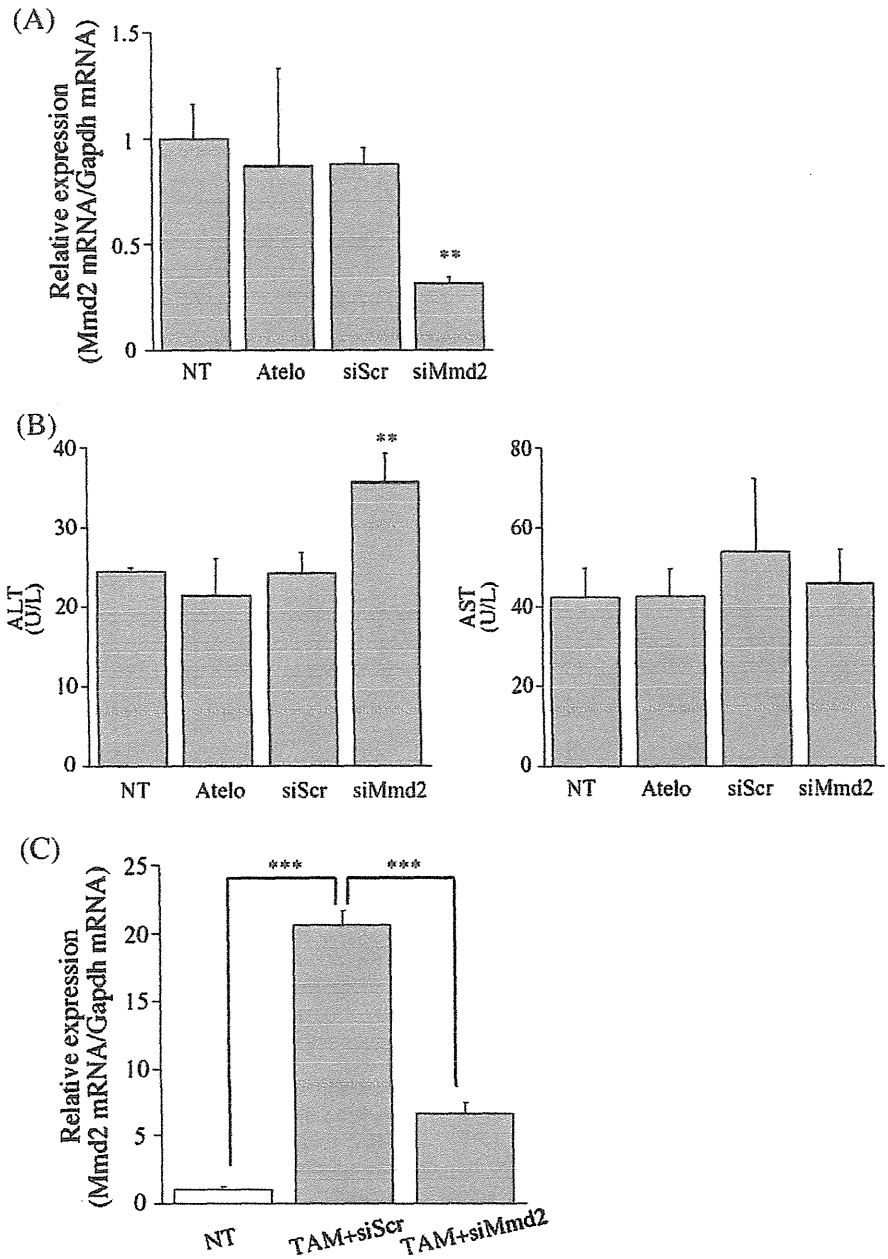

Fig. 6. The effects of siMmd2 treatment on the expression levels of hepatic Mmd2 mRNA and plasma ALT and AST in TAM-untreated and TAM-treated mice. (A, B) Atelocollagen only (Atelo), atelocollagen/siScr (siScr), or atelocollagen/siMmd2 (siMmd2) (5 nmol/mouse) in a 200-μL volume was injected into the tail vein. Plasma and liver samples were collected 24 h after the atelocollagen injection for assessment of the expression levels of Mmd2 mRNA (A) and the transaminase levels (B). (C) Mice (6 weeks old) were pretreated with TAM (1 mg/kg, *i.p.*) for 4 days. Twelve hours after the treatment of TAM, siScr or siMmd2 was injected into the tail vein. After 12 h, the last administration of TAM (1 mg/kg, *i.p.*) was performed. Liver samples were collected 12 h after the last TAM administration, and the expression levels of hepatic Mmd2 mRNA were measured. Data are shown as the mean ± SD of the results from 4 mice. Differences compared with the siScr-injected mice were considered significant at $^{**}P<0.01$, and $^{***}P<0.001$.

wildtype mice (Fig. 5), which might be one of the reasons why more severe toxicity can be observed in the ERα-knockout mice compared with the wildtype mice. Another study that used an ischemia –reperfusion mouse model demonstrated that the plasma ALT level in ERα-knockout mice was significantly higher than the ALT level in wildtype mice (Yamamoto et al., 2006). Harada et al. (2001, 2004) reported that eNOS mRNA in ERα-knockout mice was lower than the level in wildtype mice, which suggested a role for eNOS in the hepatoprotective functions of ERα. We measured the expression level of eNOS mRNA in TAM-pretreated mice that received TA and in mice that received TA alone and did not find any difference (data not shown), which suggests that eNOS was not involved in the hepatoprotective effects of TAM in mice. In addition, the expression level of eNOS mRNA was not changed by siMmd2-injection (data not shown), which suggests that Mmd2 is not likely to be involved in the regulation of eNOS expression. Based on these results, we can conclude that the hepatoprotective effect of TAM is independent of the eNOS functions.

In general, degradation of siRNA by serum nuclease is rapid. To overcome this issue, we used atelocollagen as the delivery medium of the siRNA. Atelocollagen demonstrates very low immunogenicity and the siRNA-atelocollagen complex is hardly degraded by serum nuclease; thus, the siRNA is efficiently delivered into various tissues, including liver, kidney, spleen, and lung (Minakuchi et al., 2004; Ochiya et al., 1999; Takeshita et al., 2005). Mmd2 mRNA is expressed

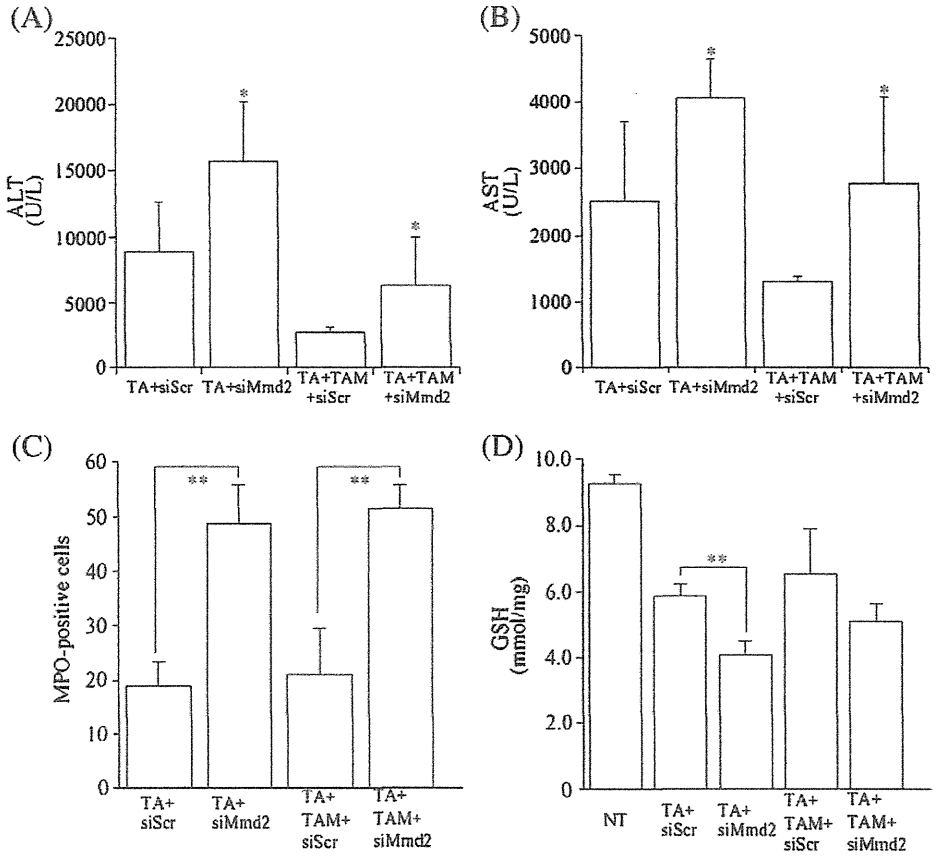

Fig. 7. The effects of siMmd2 treatment on TA-induced hepatotoxicity in mice. The mice (6 weeks old) were pretreated with TAM (1 mg/kg, *i.p.*) for 4 days. Twelve hours after the last TAM treatment, siScr or siMmd2 (5 nmol/mouse, *i.v.*) in a 200 μL volume was injected into the tail vein. Twelve hours after the siScr or siMmd2 treatment, the TAM treatment (1 mg/kg, *i.p.*) was performed. Twenty-four hours after the siScr or siMmd2 treatment, mice were administered TA (200 mg/kg, *i.p.*), and plasma was collected 24 h after the TA administration. The effects of siMmd2 treatment on the number of MPO-positive cells (C) and the GSH levels (D) in the livers of female mice are shown. Data are shown as the mean ± SD of the results from 6 mice. Differences compared with the siScr-injected mice were considered significant at $^{*}P<0.05$ and $^{**}P<0.01$.

in the liver, but not in the kidney, spleen, or lung (data not shown); thus, we confirmed that siMmd2 could decrease the Mmd2 mRNA level in the liver.

The plasma ALT and AST levels were significantly increased by siMmd2 injection compared with siScr injection in the mice that were administered TA (Fig. 7). The decreased plasma ALT and AST levels induced by TAM-pretreatment were also significantly increased by siMmd2 injection. Taken together, these results suggest that Mmd2 is involved in the exacerbation of drug-induced and chemical-induced liver injuries. The present data also suggested that siMmd2 significantly decreased the hepatic GSH levels and increased the number of MPO-positive cells (Fig. 7). GSH scavenges reactive metabolites of drug and chemicals and plays a critical role in detoxification in several types of liver injury (Yuan and Kaplowitz, 2009). In addition, MPO-positive cells are involved in immune-mediated hepatotoxicity (You et al., 2006). Therefore, the decreased GSH level suggested that there would be increased production of reactive intermediates, and the increased number of MPO-positive cells suggested an acceleration of neutrophilic infiltration. However, when we measured basal GSH levels in liver of mice administered siMmd2 alone, GSH levels were not changed (date not shown). Thus, we considered that Mmd2 might be not directly involved in the regulation of GSH levels and immune-mediated drug-induced and chemical-induced liver injuries.

Based on our novel finding that Mmd2 played an essential role in drug-induced and chemical-induced liver injuries in mice, one may surmise that MMD2 in human may also have a hepatoprotective function in the liver. The homology of the amino acid sequence between mouse Mmd2 and human MMD2 is 94%, which suggests a similar function. It is difficult to investigate the function of MMD2 in human, because MMD2 is only expressed in the liver and because substrates or biomarkers to assess the expression level of MMD2 have not been elucidated. In human liver, MMD2 mRNA was hardly expressed (Fig. 8). Furthermore, we investigated the inducibility of MMD2 by TAM and RAL (10 μM) in

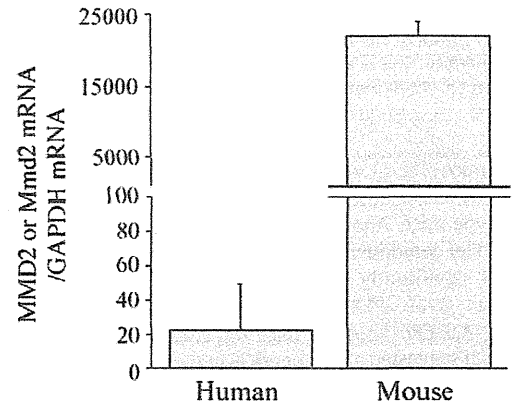

Fig. 8. The expression levels of hepatic mRNA of human MMD2 or mouse Mmd2. Data are shown as the mean ± SD of the results of liver samples from 15 human or 6 TAM-untreated mice.

primary human hepatocytes (Supplementary Fig. 4). MMD2 mRNA was increased by TAM (14.7-fold) and RAL (16.3-fold) treatment. Although the fold induction of MMD2 by RAL and TAM were similar degree of that of mouse Mmd2 (Fig. 5), large differences of expression levels were still observed between mouse and human.

The present study demonstrated that TAM has hepatoprotective effects against liver injury caused by various hepatotoxic drugs and chemicals. The present results also suggest that the protective effects of TAM are mediated by increased Mmd2 expression and a subsequent increase in GSH-mediated scavenging of reactive intermediates, which decreases hepatic inflammation. The present study provides a novel insight into the underlying mechanism for the onset of drug-induced and chemical-induced liver injuries.

Supplementary data to this article can be found online at http://dx.doi.org/10.1016/j.taap.2012.06.023.

Funding information

Health and Labor Sciences Research Grants from the Ministry of Health, Labor, and Welfare of Japan (H23-BIO-G001).

Conflict of interest statement

None of the authors have any conflicts of interest related to this manuscript.

Acknowledgments

We thank Drs. M. Takamiya and Y. Aoki (Iwate Medical University, Morioka, Japan) for supplying the human liver samples.

References

Bajt, M.L., Yan, H.M., Farhood, A., Jaeschke, H., 2008. Plasminogen activator inhibitor-1 limits liver injury and facilitates regeneration after acetaminophen overdose. Toxicol. Sci. 104, 419–427.

Behjati, S., Frank, M.H., 2009. The effects of tamoxifen on immunity. Curr. Med. Chem. 16, 3076–3080.

Cantoni, L., Valaperta, R., Ponsoda, X., Castell, J.V., Barelli, D., Rizzardini, M., Mangolini, A., Hauri, L., Villa, P., 2003. Induction of hepatic heme oxygenase-1 by diclofenac in rodents: role of oxidative stress and cytochrome P-450 activity. J. Hepatol. 38, 776–783.

Cosman, F., Lindsay, R., 1999. Selective estrogen receptor modulators: clinical spectrum. Endocr. Rev. 20, 418–434.

Dyroff, M.C., Neal, R.A., 1981. Identification of the major protein adduct formed in rat liver after thioacetamide administration. Cancer Res. 41, 3430–3435.

Early Breast Cancer Trialists' Collaborative Group (EBCTCG), 2005. Effects of chemotherapy and hormonal therapy for early breast cancer on recurrence and 15-year survival: an overview of the randomised trials. Lancet 365, 1687–1717.

Ganey, P.E., Luyendyk, J.P., Newport, S.W., Eagle, T.M., Maddox, J.F., Mackman, N., Roth, R.A., 2007. Role of the coagulation system in acetaminophen-induced hepatotoxicity in mice. Hepatology 46, 1177–1186.

Griffith, O.W., 1980. Determination of glutathione and glutathione disulfide using glutathione reductase and 2-vinylpyridine. Anal. Biochem. 106, 207–212.

Gunawan, B.K., Liu, Z.X., Han, D., Hanawa, N., Gaarde, W.A., Kaplowitz, N., 2006. c-Jun N-terminal kinase plays a major role in murine acetaminophen hepatotoxicity. Gastroenterology 131, 165–178.

Harada, H., Pavlick, K.P., Hines, I.N., Hoffman, J.M., Bharwani, S., Gray, L., Wolf, R.E., Grisham, M.B., 2001. Selected contribution: effects of gender on reduced-size liver ischemia and reperfusion injury. J. Appl. Physiol. 91, 2816–2822.

Harada, H., Bharwani, S., Pavlick, K.P., Korach, K.S., Grisham, M.B., 2004. Estrogen receptor-α, sexual dimorphism and reduced-size liver ischemia and reperfusion injury in mice. Pediatr. Res. 55, 450–456.

Kang, J.S., Wanibuchi, H., Morimura, K., Wongpoomchai, R., Chusiri, Y., Gonzalez, F.J., Fukushima, S., 2008. Role of CYP2E1 in thioacetamide-induced mouse hepatotoxicity. Toxicol. Appl. Pharmacol. 228, 295–300.

Koen, Y.M., Williams, T.D., Hanzlik, R.P., 2000. Identification of three protein targets for reactive metabolites of bromobenzene in rat liver cytosol. Chem. Res. Toxicol. 13, 1326–1335.

Kuiper, G.G., Carlsson, B., Grandien, K., Enmark, E., Häggblad, J., Nilsson, S., Gustafsson, J.A., 1997. Comparison of the ligand binding specificity and transcript tissue distribution of estrogen receptors α and β. Endocrinology 138, 863–870.

Kumada, T., Tsuneyama, K., Hatta, H., Ishizawa, S., Takano, Y., 2004. Improved 1-h rapid immunostaining method using intermittent microwave irradiation: practicability based on 5 years application in Toyama Medical and Pharmaceutical University Hospital. Mod. Pathol. 17, 1141–1149.

McGovern, D.P., Jones, M.R., Taylor, K.D., Marciante, K., Yan, X., Dubinsky, M., Ippoliti, A., Vasiliauskas, E., Berel, D., Derkowski, C., Dutridge, D., Fleshner, P., Shih, D.Q., Melmed, G., Mengesha, E., King, L., Pressman, S., Haritunians, T., Guo, X., Targan, S.R., Rotter, J.I., International IBD Genetics Consortium, 2010. Fucosyltransferase 2 (FUT2) non-secretor status is associated with Crohn's disease. Hum. Mol. Genet. 19, 3468–3476.

Minakuchi, Y., Takeshita, F., Kosaka, N., Sasaki, H., Yamamoto, Y., Kouno, M., Honma, K., Nagahara, S., Hanai, K., Sano, A., Kato, T., Terada, M., Ochiya, T., 2004. Atelocollagen-mediated synthetic small interfering RNA delivery for effective gene silencing in vitro and in vivo. Nucleic Acids Res. 32, e109.

Mitlak, B.H., Cohen, F.J., 1997. In search of optimal long-term female hormone replacement: the potential of selective estrogen receptor modulators. Horm. Res. 48, 155–163.

Morita, M., Akai, S., Hosomi, H., Tsuneyama, K., Nakajima, M., Yokoi, T., 2009. Drug-induced hepatotoxicity test using γ-glutamylcysteine synthetase knockdown rat. Toxicol. Lett. 189, 159–165.

Naugler, W.E., Sakurai, T., Kim, S., Maeda, S., Kim, K., Elsharkawy, A.M., Karin, M., 2007. Gender disparity in liver cancer due to sex differences in MyD88-dependent IL-6 production. Science 317, 121–124.

Nazari-Shafti, T.Z., Freishinger, E., Roy, U., Bulot, C.T., Senst, C., Duplin, C.L., Chaffin, A.E., Srivastava, S.K., Mondal, D., Alt, E.U., Izadpanah, R., 2011. Mesenchymal stem cell derived hematopoietic cells are permissive to HIV-1 infection. Retrovirology 8, 3–14.

Numata, K., Kubo, M., Watanabe, H., Takagi, K., Mizuta, H., Okada, S., Kunkel, S.L., Ito, T., Matsukawa, A., 2007. Overexpression of suppressor of cytokine signaling-3 in T cells exacerbates acetaminophen-induced hepatotoxicity. J. Immunol. 178, 3777–3785.

Ochiya, T., Takahama, Y., Nagahara, S., Sumita, Y., Hisada, A., Itoh, H., Nagai, Y., Terada, M., 1999. New delivery system for plasmid DNA in vivo using atelocollagen as a carrier material: the Minipellet. Nat. Med. 5, 707–710.

Osborne, C.K., Fuqua, S.A., 1994. Mechanisms of tamoxifen resistance. Breast Cancer Res. Treat. 32, 49–55.

Porter, W.R., Gudzinowicz, M.J., Neal, R.A., 1979. Thioacetamide-induced hepatic necrosis. II. Pharmacokinetics of thioacetamide and thioacetamide-S-oxide in the rat. J. Pharmacol. Exp. Ther. 208, 386–391.

Purcell, P., Henry, D., Melville, G., 1991. Diclofenac hepatitis. Gut 32, 1381–1385.

Randle, L.E., Goldring, C.E.P., Benson, C.A., Metchalfe, P.N., Kitteringham, N.R., Park, B.K., Williams, D.P., 2008. Investigation of the effect of a panel of model hepatotoxins on the Nrf2-Keap1 defence response pathway in CD-1 mice. Toxicology 243, 249–260.

Takeshita, F., Minakuchi, Y., Nagahara, S., Honma, K., Sasaki, H., Hirai, K., Teratani, T., Namatame, N., Yamamoto, Y., Hanai, K., et al., 2005. Efficient delivery of small interfering RNA to bone-metastatic tumors by using atelocollagen in vivo. Proc. Natl. Acad. Sci. U. S. A. 102, 12177–12182.

Yamamoto, Y., Moore, R., Hess, H.A., Guo, G.L., Gonzalez, F.J., Korach, K.S., Maronpot, R.R., Negishi, M., 2006. Estrogen receptor α mediates 17α-ethynylestradiol causing hepatotoxicity. J. Biol. Chem. 281, 16625–16631.

You, Q., Cheng, L., Reilly, T.P., Wegmann, D., Ju, C., 2006. Role of neutrophils in a mouse model of halothane-induced liver injury. Hepatology 44, 1421–1431.

Yuan, L., Kaplowitz, N., 2009. Glutathione in liver diseases and hepatotoxicity. Mol. Aspects Med. 30, 29–41.

Drug Metab. Pharmacokinet. 27 (6): 621–630 (2012).

Regular Article

Stimulation of Human Monocytic THP-1 Cells by Metabolic Activation of Hepatotoxic Drugs

Shinya ENDO, Yasuyuki TOYODA, Tatsuki FUKAMI, Miki NAKAJIMA and Tsuyoshi YOKOI*

Drug Metabolism and Toxicology, Faculty of Pharmaceutical Sciences, Kanazawa University, Kanazawa, Japan

Full text of this paper is available at http://www.jstage.jst.go.jp/browse/dmpk

Summary: Drug-induced liver injury (DILI) is thought to be involved in the participation of drugs that either directly affect the cell viability or elicit an immune response. However, there is limited information about the immune responses induced by drugs, including those drugs that are metabolically activated. In this study, we constructed an *in vitro* assay system to assess the involvement of immune-related factors induced by metabolic activation of drugs. To investigate whether CYP3A4-mediated metabolism of 10 hepatotoxic drugs is associated with immune-related responses, human monocytic leukemia THP-1 cells were co-incubated with CYP3A4 Supersomes. Cluster of differentiation (CD) 86 and CD54 expression levels on THP-1 cells were upregulated by treatment with albendazole and amiodarone (AMD), respectively, in the presence of CYP3A4. Additionally, *N*-desethylamiodarone (DEA), a major metabolite of AMD, upregulated the CD54 expression of THP-1 cells with CYP3A4. The release of interleukin (IL)-8 and tumor necrosis factor (TNF) α from THP-1 cells was significantly increased by the treatment of AMD or DEA with CYP3A4. Similarly, IL-8 and TNFα were also upregulated by the treatment of AMD and DEA with human liver microsomes, but were inhibited by adding ketoconazole to the cell culture. In this study, we first report that albendazole, AMD and DEA activate immune reaction when metabolically activated.

Keywords: adverse drug reactions; bioactivation; monocytes/macrophages; CYP3A4; drug-induced hepatotoxicity; inflammation

Introduction

Drug-induced liver injury (DILI) is a rare but serious adverse reaction to a large number of pharmaceutical drugs and the most common reason for restrictions or withdrawal from the market. Most such drugs are known to produce reactive metabolites after metabolic activation.[1] It has been suggested that activation of the innate immune system by metabolic activation of drugs is involved in the pathogenesis of the immune-mediated drug-induced liver injury as one of the causes.[2–4]

Cytochrome P450 (CYP) plays a prominent role in metabolic activation, resulting in the generation of a reactive metabolite. One of the CYP isoforms, CYP3A4, is the predominant isoform in liver and metabolizes more than 50% of the clinical drugs commonly used.[5] On the other hand, CYP3A4 is one of the important enzymes involved in the metabolic activation of various drugs causing drug-induced liver injury.[6]

There have been some reports about the immune responses caused by metabolic activation of drugs. For example, it has been reported that halothane is metabolized to trifluoroacetyl radicals by CYP2E1 and these covalently bind to target macromolecules.[7] Sulfamethoxazole and its reactive metabolite nitroso sulfamethoxazole stimulate dendritic cells, resulting in the generation of co-stimulatory signals required to initiate a primary immune response.[8] However, such drugs causing immune response after metabolic activation remain largely undefined.

Recently, the involvement of the immune system in drug-induced liver injury has been suggested using *in vivo* mouse models.[9–14] Inflammatory reactions in the liver are induced by the activation of innate immune cells, such as monocytes, macrophages and Kupffer cells. Activated monocytes and

Received February 6, 2012; Accepted May 21, 2012
J-STAGE Advance Published Date: June 12, 2012, doi:10.2133/dmpk.DMPK-12-RG-019
**To whom correspondence should be addressed:* Tsuyoshi YOKOI, Ph.D., *Drug Metabolism and Toxicology, Faculty of Pharmaceutical Sciences, Kanazawa University, Kakuma-machi, Kanazawa 920-1192, Japan. Tel. +81-76-234-4407, Fax. +81-76-234-4407, E-mail: tyokoi@p.kanazawa-u.ac.jp*
This work was supported in part by Research on Advanced Medical Technology, Health and Labour Sciences Research from the Ministry of Health, Labour and Welfare of Japan [Grant H23-BIO-G001].

macrophages release large amounts of pro-inflammatory cytokines and chemokines, including tumor necrosis factor (TNF) α and interleukin (IL)-8. TNFα triggers the release of a cascade of other cytokines that recruit and activate lymphocytes and macrophages.[15] IL-8 exhibits multiple effects on neutrophils, including the induction of lysosomal enzyme release, increase in the expression of adhesion molecules, and rapid infiltration.[16,17] In a mouse model of halothane-induced liver injury, it was shown that the production of TNFα, IL-1β, IL-6 and IL-8 and neutrophil infiltration in liver play a critical role in immune-mediated liver injury.[18]

In recent years, human monocytic cell lines have been used to examine the inflammatory responses mediated by drugs withdrawn from the market. In human monocytic THP-1 cells, the mRNA expression levels and/or the release of pro-inflammatory cytokines and chemokines were increased by treatment with troglitazone or ximelagatran.[19,20] Additionally, our previous research revealed that albendazole and terbinafine also stimulate THP-1 cells resulting in IL-8 and TNFα release, suggesting the mechanism of immune-mediated liver injury.[21,22] Therefore, THP-1 cells would be useful to predict immune responses by drugs.

In this study, we investigated whether bioactivation of hepatotoxic drugs stimulates THP-1 cells resulting in the upregulation of the cell surface markers cluster of differentiation (CD) 86 and CD54 and the release of pro-inflammatory cytokines and chemokines from THP-1 cells in the presence or absence of CYP3A4 or human liver microsomes (HLM).

Materials and Methods

Materials: Albendazole and nitrofurantoin were obtained from Sigma-Aldrich (St. Louis, MO). Albendazole sulfoxide was obtained from Toronto Research Chemicals (Ontario, Canada). β-NADPH was from Oriental Yeast (Tokyo, Japan). Diclofenac, desipramine, nefazodone, tacrine and terbinafine were from Wako Pure Chemicals (Osaka, Japan). AMD and leflunomide were obtained from LKT Labs (St. Paul, MN) and Alexis Biochemicals (San Diego, CA), respectively. DEA (2-butyl-3-benzofuranyl 4-[2-(monoethylamino)ethoxy]-3,5-diiodophenyl ketone, a main metabolite of AMD) was kindly provided by Taisho Pharmaceutical (Tokyo, Japan). Human CYP3A4 Supersomes (recombinant cDNA-expressed P450 enzymes prepared from a baculovirus insect cell system) (testosterone 6β-hydroxylase activity is 22,059 pmol/mg × min) and control Supersomes and pooled HLM (n = 50, testosterone 6β-hydroxylase activity is 5,700 pmol/mg × min) were purchased from BD Gentest (Woburn, MA). The specific catalytic activities of each CYP isoform in these microsomes were provided by the manufacturer. Primers were commercially synthesized at Hokkaido System Sciences (Sapporo, Japan). All other reagents were of the highest grade commercially available.

Cell culture and drug treatment: Human monocytic leukemia cell line THP-1 was obtained from Riken Gene Bank (Tsukuba, Japan). THP-1 cells were cultured in RPMI 1640 medium (Nissui Pharmaceutical, Tokyo, Japan) supplemented with 10% fetal bovine serum (FBS; Invitrogen, Carlsbad, CA), and were maintained at 37°C under an atmosphere of 5% CO_2. THP-1 cells were seeded at a density of 1×10^6 cells/well in 24-well plates with the medium containing the indicated concentration of the drugs and 1 mM β-NADPH and 15 nM human CYP3A4 Supersomes, or control Supersomes or 0.3 mg/mL microsomal protein of human livers and then incubated at 37°C. The selected drugs have all been shown to be substrates of CYP3A4, albeit not exclusive to CYP3A4. The final concentration of dimethyl sulfoxide (DMSO) in the medium was 0.1%. Heat-inactivated (treated at 56°C for 30 min) HLM were used as a control.

Flow cytometry using monoclonal antibodies (mAbs): The expression of CD86 and CD54 on the THP-1 cells was measured as previously described with some modifications.[23] In brief, cells were harvested 24 h after the treatment and washed twice with fluorescence-activated cell sorting (FACS) buffer (phosphate-buffered saline containing 1% bovine serum albumin). Cell surface staining was performed using the following flourescein isothiocyanate (FITC)-conjugated monoclonal antibodies (mAbs): anti-human CD54 (clone; 6.5B5) from DAKO (Glostrup, Denmark), anti-human CD86 (clone; Fun-1) from BD Pharmingen (San Diego, CA); and FITC-labeled mouse IgG_1 (clone; MOPC-21) from BD Pharmingen. Cells were incubated with the above mAbs at 6 µl/3×10^5 cells/50 µl for anti-human CD54 mAb. In addition, FITC-labeled mouse IgG_1 as an isotype control was used at a dilution of 3 µl/3×10^5 cells/50 µl. Cells were incubated with these mAbs for 30 min at 4°C. After washing and resuspension with FACS buffer, the surface marker expression was measured and analyzed using FACSCalibur and Cell Quest Pro software (BD Biosciences, San Jose, CA). Propidium iodide (PI) was used at a concentration of 0.625 µg/mL, after which dead cells were gated out and the mean fluorescence intensity for each marker was recorded for a total of 10,000 living cells. The relative mean fluorescence intensity represented as percentage was calculated by taking the ratios of the mean fluorescence intensity of treated cells to that of controls. Cell viability was determined by the PI assay. If cell viability was less than 50%, the expression levels of this tested concentration was not calculated and included in the evaluation because of diffuse labeling cytoplasmic structures due to cell membrane destruction.[24]

Enzyme-linked immunosorbent assay (ELISA): The pro-inflammatory cytokine TNFα and the chemokine IL-8 are reported to be sensitive markers in THP-1 cells.[21,22,25] TNFα and IL-8 in cell supernatants were measured by Human TNFα or IL-8 ELISA Ready-SET-GO!™

(eBioscience, San Diego, CA) according to the manufacturer's instructions.

Real-time reverse transcription-polymerase chain reaction (RT-PCR): Total RNA was extracted from THP-1 cells with RNAiso (Takara Bio, Shiga, Japan) according to the protocol supplied by manufacturer. The primers used in this study were human IL-8 (forward: 5′-CAGCCTTCCTGATTTCTCTGCAG-3′, reverse: 5′-AGACAGAGCTCTCTTCCATCAG-3′) and human TNFα (forward: 5′-CTTCTGCCTGCTGCACTTTGGAG-3′, reverse: 5′-GGCTACAGGCTTGTCACTCGG-3′). The IL-8 and TNFα mRNA levels were normalized with human glyceraldehyde 3-phosphate dehydrogenase (GAPDH) mRNA (forward: 5′-CCATGAGAAGTATGACAACAGCC-3′, reverse: 5′-TGGGTGGCAGTGATGGCATGGA-3′). The reverse transcription process and real-time RT-PCR were performed as described previously.[12]

Quantification of AMD, DEA and DiDEA using high-performance liquid chromatography (HPLC): Quantification of AMD and DEA was performed according to our previous method with slight modifications.[26] After treatment with 30 μM AMD or 20 μM DEA in the presence or absence of CYP3A4 for 12 and 24 h, 5 μM tolbutamide as an internal standard (IS) was added after the incubation and the THP-1 cells were collected. Cells were lysed by three freeze-thaw cycles. The reaction mixture was extracted with 4 mL of dichloromethane for 1 min. The organic layer was transferred to a clean test tube and was evaporated under a gentle stream of nitrogen at 40°C. The residue was redissolved in 100 μl of mobile phase, and an 80-μl portion was subjected to HPLC. HPLC analysis was performed using an L-7100 pump (Hitachi, Tokyo, Japan), 712 WISP intelligent sample processor (Waters, Tokyo, Japan), Chromatointegrator D-2000 (Hitachi), and CTO-6A column oven (Shimadzu, Kyoto, Japan) with a Capcell Pak CN UG120 (4.6 × 150 mm; 5 mm) column (Shiseido, Tokyo, Japan). The eluent was monitored at 240 nm using an SPD-6A UV detector (Shimadzu). The mobile phase was 32% acetonitrile, 1% acetic acid, and 0.2% diethylamine. The flow rate was 1.0 mL/min, and the column temperature was 35°C. Under these conditions, retention times of IS, di-*N*-desethylamiodarone (DiDEA), DEA and AMD were 3.5, 6.5, 9.5, and 13.0 min, respectively.

Cell viability assay: Cell viability was evaluated by the PI assay. After incubation, cells were washed twice with FACS buffer, then stained with PI (0.625 μg/mL), and the cell viability was measured using FACSCalibur and Cell Quest Pro software (BD Biosciences). Total events for living cell counting were 10,000.

Statistical analysis: Data are expressed as mean ± SD. Comparison of 2 groups was made with an unpaired, two-tailed Student's *t*-test. Comparison of multiple groups was made with ANOVA followed by a Dunnett or Tukey test. A value of $p < 0.05$ was considered statistically significant.

Table 1. Effects of various hepatotoxic drugs on cell viability of THP-1 cells in the PI assay

Drug	Concentration (μM)	Cell viability (%)	
		CYP3A4 (−)	CYP3A4 (+)
0.1% DMSO	—	100.0 ± 1.5	100.0 ± 2.0
Albendazole	50	84.3 ± 2.1	84.7 ± 3.0
Albendazole sulfoxide	50	85.9 ± 2.6	87.4 ± 2.5
Amiodarone	30	90.4 ± 8.5	71.7 ± 10.6
Desethylamiodarone	20	91.6 ± 2.3	87.8 ± 1.4
Desipramine	30	97.3 ± 3.1	95.2 ± 2.8
Diclofenac	100	90.7 ± 1.8	89.8 ± 2.5
Hydralazine	100	81.0 ± 2.7	78.3 ± 3.4
Leflunomide	20	98.7 ± 2.3	97.3 ± 1.4
Nefazodone	10	97.5 ± 2.4	99.1 ± 1.5
Tacrine	100	100.9 ± 1.4	98.3 ± 1.2
Tamoxifen	20	88.1 ± 5.5	88.5 ± 5.1
Terbinafine	100	77.5 ± 5.7	80.4 ± 6.4

Data represent the mean ± SD ($n = 3$).

Results

Effect of CYP3A4 on various hepatotoxic drugs assessed by the expression of CDs in human monocytic THP-1 cells: To investigate whether metabolic activation of hepatotoxic drugs affects human monocytic cells, THP-1 cells were treated with the indicated concentrations (Table 1) of various hepatotoxic drugs for 24 h in the presence or absence of CYP3A4 Supersomes and then the expressions of CD86 and CD54 on the THP-1 cells were measured by FACS. The cell viability of THP-1 cells treated with these drugs was 70% or more (Table 1), which is consistent with the other report.[27] In the presence of CYP3A4, CD86 expression in THP-1 cells was significantly increased by the treatment with albendazole compared with control Supersomes but not by treatment with albendazole sulfoxide, the active metabolite of albendazole (Fig. 1A).[28] The CD54 expression in THP-1 cells was significantly increased by the treatment with AMD and DEA, active metabolites of AMD, in the presence of CYP3A4, compared with control Supersomes (Fig. 1B). None of the other hepatotoxic drugs showed the effect of CYP3A4 metabolism on the expression of CD86 and CD54. These results suggested that albendazole, AMD and DEA have the ability to increase the CD expression levels leading to the activation of the immune responses. For the subsequent studies, the CYP3A4-dependent metabolism of AMD and DEA was focused on because AMD showed the highest activation and the major metabolite of AMD also activates the CD of THP-1 cells.

Dose-dependent changes of the CD54 expression in THP-1 cells treated with AMD or DEA in the presence or absence of CYP3A4: To investigate whether CYP3A4-dependent metabolism of AMD and DEA at low concentrations can affect the CD54 expression, THP-1 cells were treated with AMD or DEA at the indicated

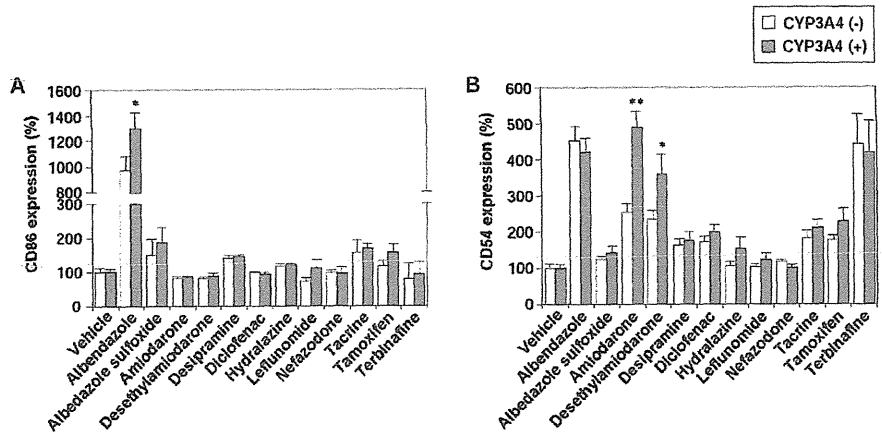

Fig. 1. Effect of CYP3A4 on various hepatotoxic drugs assessed by the expression of CD86 and CD54 in THP-1 cells
THP-1 cells were treated with 50 μM albendazole, 50 μM albendazole sulfoxide, 30 μM AMD, 20 μM DEA, 30 μM desipramine, 100 μM diclofenac, 100 μM hydralazine, 20 μM leflunomide, 10 μM nefazodone, 100 μM tacrine, 20 μM tamoxifen or 100 μM terbinafine for 24 h in the presence or absence of CYP3A4 (15 pmol/mL). After the incubation, the expression levels of CD86 (A) and CD54 (B) was measured by flow cytometry. CD expression levels are expressed as percentage of vehicle (0.1% DMSO)-treated cells. Data represent the mean ± SD ($n = 3$). *$p < 0.05$ and **$p < 0.001$, compared with each CYP3A4 (−) group.

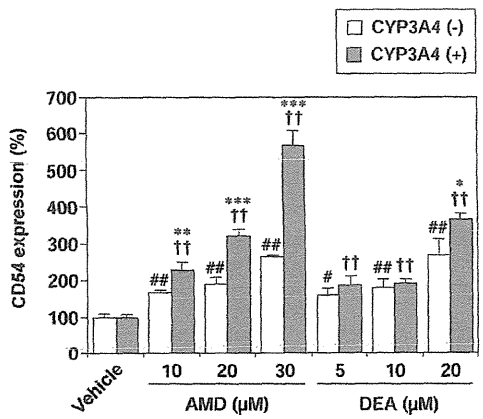

Fig. 2. Dose-dependent changes of the CD54 expression in THP-1 cells treated with AMD or DEA in the presence or absence of CYP3A4
THP-1 cells were treated with the indicated concentration of AMD and DEA for 24 h in the presence or absence of CYP3A4 (15 pmol/mL). CD expression level is expressed as percentage of vehicle-treated cells. Data represent the mean ± SD ($n = 3$). #$p < 0.05$ and ##$p < 0.01$, compared with control (0.1% DMSO) in CYP3A4 (−) groups; ††$p < 0.01$, compared with control (0.1% DMSO) in CYP3A4 (+) groups; *$p < 0.05$, **$p < 0.01$ and ***$p < 0.001$, compared with CYP3A4 (−) groups at each concentration.

concentration for 24 h in the presence or absence of CYP3A4, and then the expression of CD54 was measured using FACS. As shown in Figure 2, AMD and DEA increased the CD54 expression in the presence of CYP3A4 compared with the control. With the CYP3A4 treatment, the expression of CD54 in THP-1 cells was significantly increased in an AMD dose-dependent manner and, to a lesser extent, increased CD54 expression induced by DEA.

Time-dependent changes of the mRNA expression and the release of IL-8 and TNFα in THP-1 cells treated with AMD or DEA in the presence or absence of CYP3A4: The time-dependent changes of the CYP3A4-dependent metabolism by AMD on the IL-8 and TNFα levels in THP-1 cells were investigated. When treated with 30 μM AMD in the presence of CYP3A4, the mRNA expression levels and the release of IL-8 and TNFα in THP-1 cells were significantly increased after incubation for 3 to 24 h compared with the control (Fig. 3). The mRNA expression levels of IL-8 were increased in a time-dependent manner, and were most increased after 12 h-incubation (Fig. 3A). The highest increase of the mRNA expression and release of TNFα was shown at 12 h- and 6 h-incubation, separately (Figs. 3B and 3D).

When treated with 20 μM DEA in the presence of CYP3A4, the mRNA expression of IL-8 was most increased at 3 h-incubation (Fig. 4A). The highest increase of the mRNA expression levels and release of TNFα was shown at 6 h-incubation (Figs. 4B and 4D). To investigate the effect of AMD metabolism, the incubation time of 12 h was selected for the subsequent study to measure the formation of AMD, DEA and DiDEA. To investigate whether there were cytotoxic effects on THP-1 cells caused by the leakage of intracellular cytokines and chemokines, a cell viability assay was performed in THP-1 cells. At 24 h-incubation, AMD and DEA had slight cytotoxic effects on the THP-1 cells (Supplemental Fig. 1).

Quantification of metabolites of AMD and DEA using HPLC: The formation of the metabolites of AMD by CYP3A4 Supersomes was measured by HPLC. The concentrations of AMD, DEA and DiDEA were determined 12 and 24 h after the treatment with 30 μM AMD (Table 2) or 20 μM DEA (Table 3) in the presence or absence of

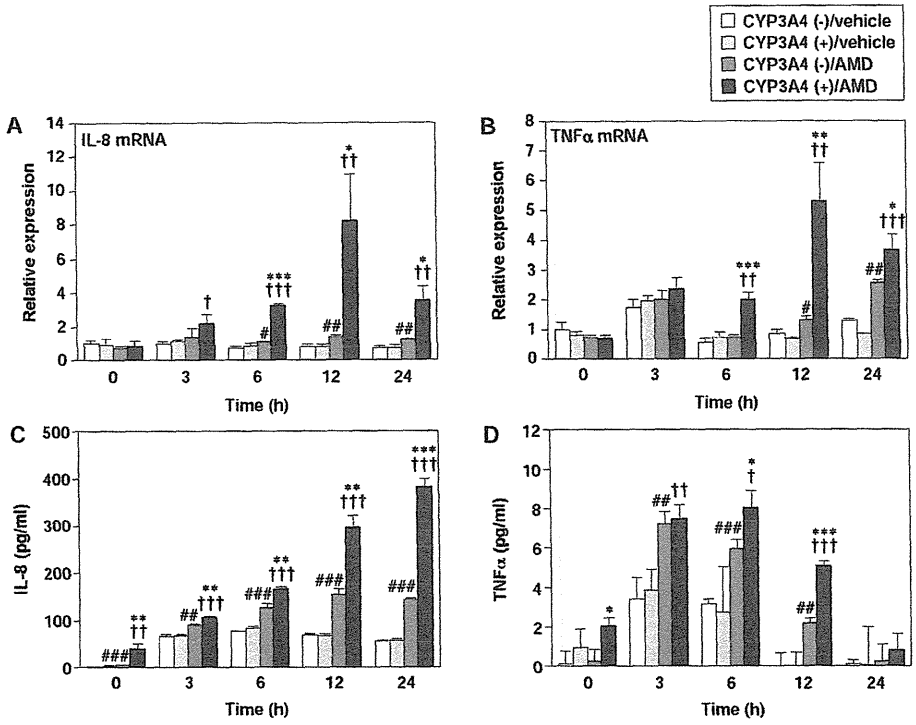

Fig. 3. Time-dependent changes in the mRNA expression and the release of IL-8 and TNFα in THP-1 cells treated with 30 μM AMD in the presence or absence of CYP3A4

THP-1 cells were treated with 30 μM AMD for 3, 6, 12, or 24 h in the presence or absence of CYP3A4 (15 pmol/mL). The mRNA expression levels of IL-8 (A) and TNFα (B) in THP-1 cells were measured by real-time RT-PCR analysis. The levels of IL-8 or TNFα mRNA were normalized to the level of GAPDH mRNA. The release of IL-8 protein (C) and TNFα protein (D) in the supernatant was measured by ELISA. Data represent the mean ± SD ($n = 3$). $^{\#\#}p < 0.01$ and $^{\#\#\#}p < 0.001$, compared with control (0.1% DMSO) in each time point of CYP3A4 (−) groups; $^{\dagger}p < 0.05$, $^{\dagger\dagger}p < 0.01$ and $^{\dagger\dagger\dagger}p < 0.001$, compared with control (0.1% DMSO) in each time point of CYP3A4 (+) groups; $^{*}p < 0.05$, $^{**}p < 0.01$ and $^{***}p < 0.001$, compared with CYP3A4 (−) groups at each time point.

Table 2. Metabolism of AMD by CYP3A4 Supersomes for 12 h- and 24 h-incubation

Time (h)	CYP3A4 (−)			CYP3A4 (+)		
	AMD (μM)	DEA (μM)	DiDEA (μM)	AMD (μM)	DEA (μM)	DiDEA (μM)
0	33.4 ± 8.0	ND	ND	26.1 ± 5.8	ND	ND
12	27.6 ± 2.1	ND	ND	18.3 ± 6.7	7.4 ± 3.8	ND
24	28.6 ± 2.6	ND	ND	17.1 ± 4.7	11.7 ± 4.5	0.4 ± 0.1

THP-1 cells were treated with 30 μM AMD for 12 and 24 h in the presence or absence of CYP3A4 (15 pmol/mL). Data represent the mean ± SD ($n = 3$). ND, not detectable.

Table 3. Metabolism of DEA by CYP3A4 Supersomes for 12 h- and 24 h-incubation

Time (h)	CYP3A4 (−)			CYP3A4 (+)		
	AMD (μM)	DEA (μM)	DiDEA (μM)	AMD (μM)	DEA (μM)	DiDEA (μM)
0	ND	16.0 ± 1.4	ND	ND	17.5 ± 3.6	ND
12	ND	19.4 ± 3.1	ND	ND	15.3 ± 5.0	0.3 ± 0.0
24	ND	19.2 ± 6.5	ND	ND	19.2 ± 6.2	0.5 ± 0.3

THP-1 cells were treated with 20 μM DEA for 12 and 24 h in the presence or absence of CYP3A4 (15 pmol/mL). Data represent the mean ± SD ($n = 3$). ND, not detectable.

CYP3A4. The metabolites of AMD, DEA and DiDEA were detected only in the presence of CYP3A4 Supersomes 24 h after AMD treatment (Table 2). DiDEA was detected in the presence of CYP3A4 Supersomes after 24 h treatment with AMD and in the presence of CYP3A4 Supersomes after 12 and 24 h treatment with DEA (Table 3). The AMD concentrations decreased time-dependently after 24 h exposure, but the DEA concentrations slightly decreased after 24 h exposure, and thus DiDEA was likely not efficiently biotransformed. In contrast, incubation with control Supersomes did not generate detectable amounts of the metabolites with either AMD or DEA.

Time-dependent changes of the mRNA expression of IL-8 and TNFα in THP-1 cells treated with AMD or DEA in the presence or absence of HLM: To investigate whether metabolic activation of AMD and DEA occurs in the presence of HLM, we measured the time-dependent changes of the mRNA expression of IL-8 and TNFα in THP-1 cells. When treated with 30 μM AMD in the presence of HLM, the mRNA expression levels of IL-8